THE EFFECTS OF TEMPERATURE, CO_2, AND NITROGEN SOURCE ON THE GROWTH AND PHYSIOLOGY OF THE RAPHIDOPHYTES *HETEROSIGMA AKASHIWO* AND *CHATTONELLA SUBSALSA*

by

Lauren Rose Salvitti

A thesis submitted to the Faculty of the University of Delaware in partial fulfillment of the requirements for the degree of Master of Marine Biosciences

Spring 2010

THE EFFECTS OF CO_2, TEMPERATURE, AND NITROGEN SOURCE ON THE GROWTH AND PHYSIOLOGY OF THE RAPHIDOPHYTES *HETEROSIGMA AKASHIWO* AND *CHATTONELLA SUBSALSA*

by
Lauren Rose Salvitti

Approved: _____
Mark E. Warner, Ph.D.
Professor in charge of thesis on behalf of the Advisory Committee

Approved: _____
Charles E. Epifanio, Ph.D.
Director of the School of Marine Science and Policy

Approved: _____
Nancy Targett, Ph.D.
Dean of the College of Earth, Ocean, and Environment

Approved: _____
Debra Hess Norris, M.S.
Vice Provost for Graduate and Professional Education

ACKNOWLEDGMENTS

I would like to acknowledge my advisor Mark Warner for all his guidance, patience and inspiration during my time here at University of Delaware and to Kathy Coyne for taking a chance with an inexperienced undergraduate and giving me the opportunity to further my science career. Also, thanks to my committee member Matt Oliver for his infectious enthusiasm and love of science. You have all provided me with invaluable advice and confidence as I take my next steps in my career.

I would also like to thank my lab mates Jen Stewart, Mike McGinley, Sebastian Hennige, Kevin Portune, Matt Aschaffenburg, and our summer intern Katie Bus, for their countless hours helping me in the lab and lending an ear. Special thanks go to Jen Stewart and Adam Pimenta for saving me from more than one catastrophe and helping me retain my sanity. Thanks to the many professors, students, and staff at University of Delaware who have lent a helping hand over the years, including Matt Butler, Stef Guida, Sara Handy, Joe Scudlark, John Sharp, Paul Dumigan, Connie Edwards, Peggy Conlon, Debbie Booth, Janis Lopez, Roseann Caraway, and all the maintenance staff. Many thanks also to my friends near and far who have always been just a phone call away. Laura Montfort, Rachel Saltz, Catherine Liebman, Ashley Gavarny, Sherri Anderson, Lauren Harner, Michael Weed, Jacquie Nicholl, and Janeen McGinley, I would have never gotten this far without your love and friendship.

Lastly, but most importantly, I'd like to thank my family... mom, dad, Matt, and Ellie. You have been my constant source of encouragement, advice, support,

and unconditional love for the past 26 years. I would never be where I am today with you and I appreciate everything you have done for me more than you know.

TABLE OF CONTENTS

LIST OF TABLES vii
LIST OF FIGURES viii
ABSTRACT xi

Chapter
1 INTRODUCTION 2

1.1 Light 5
1.2 Temperature 7
1.3 Nutrients 8
1.4 Carbon 10
1.5 Model Species 13

2 THE IMPACT OF LONG-TERM SHIFTS IN CO_2 AND TEMPERATURE ON THE GROWTH AND PHYSIOLOGY OF *HETEROSIGMA AKASHIWO* AND *CHATTONELLA SUBSALSA* 16

ABSTRACT 16
2.1 INTRODUCTION 17
2.2 METHODS AND MATERIALS 23

2.2.1 Isolates and culture conditions 23
2.2.2 Experimental design 23
2.2.3 Growth rates, Chlorophyll *a*, and fluorescence measurements 24
2.2.4 Determination of P:E curves, primary production, and light absorption 26
2.2.5 Dissolved inorganic carbon and partial pressure of CO_2 30
2.2.6 Statistics 30

2.3 RESULTS 31

2.3.1 Growth and carbon assimilation 31
2.3.2 Chlorophyll fluorescence 34

2.4 DISCUSSION 39

3 THE POTENTIAL USE OF THE NITRATE REDUCTION PATHWAY AS A DISSAPATING MECHANISM FOR EXCESS EXCITATION ENERGY IN THE RAPHIDOPHYTE *HETEROSIGMA AKASHIWO* 49

ABSTRACT 49
3.1 INTRODUCTION 50
3.2 METHODS 53

3.2.1 Isolates and culture conditions 53
3.2.2 Experimental design 53
3.2.2 Fluorescence analysis 54
3.2.3 Statistics 56

3.3 RESULTS AND DISCUSSION 57
3.4 CONCLUSIONS 66

APPENDIX 70
BIBLIOGRAPHY 79

LIST OF TABLES

Table 2.1 Chlorophyll fluorescence parameters as measured by Fluorescence Induction and Relaxation (FIRe) fluorometery 29

Table 3.1 ETR_{max} of *H. akashiwo* grown with either nitrate or ammonium as a nitrogen source and with or without continuous aeration..... 58

Table A.1 Measured and calculated growth and carbon chemistry parameters under each of the four temperature/CO_2 treatments. Different letters denote significant difference (numbers in parenthesis = S.D. with $n \geq 3$). 71

Table A.2 Significant ($p < 0.05$) intraspecific differences between control, high temperature, high CO_2, and combined treatments..... 73

Table A.3 Significant ($p < 0.05$) interspecific differences between *Heterosigma akashiwo* (DIB), *Heterosigma akashiwo* (WA), and *Chattonella subsalsa* (DIB) grown under four treatments: 'Control' (25 °C + 375 ppm CO_2), 'High CO_2' (25 °C + 750 ppm CO_2), 'High Temperature' (30 °C + 375 ppm CO_2), 'Combined' (30 °C + 750 ppm CO_2). 74

Table A.4 Measured and calculated parameters of low biomass (LB) or high biomass (HB) *H. akashiwo* (DIB) cultures bubbled with ambient air (375ppm) or high CO_2 (750ppm) and grown at 25 °C . Different letters denote significant difference (numbers in parentheses = S.D, n = 3). 78

LIST OF FIGURES

Figure 2.1 Cell specific growth rates (A), maximal photosynthesis (B), photosynthetic efficiency (C), and primary productivity (D) of *H. akashiwo* (DIB), *H. akashiwo* (WA) and *C. subsalsa* (DIB) in the four temperature and CO_2 treatments. Error bars denote standard deviation (n = 3) and different letters represent significant difference within each strain ($p < 0.05$). 33

Figure 2.2 Maximal quantum efficiency of PSII (A), functional absorption cross section (B), connectivity (C), rate of PSII reoxidation (D) in *H. akashiwo* (DIB), *H. akashiwo* (WA), and *C. subsalsa* (DIB). Error bars denote standard deviation (n = 3) and different letters represent significant difference within algal strain (One-way ANOVA, $p < 0.05$). Note: F_v/F_m and σ_{PSII} were analyzed with FIRePro and ρ and Tau were analyzed with FIReWorx. 36

Figure 2.3 Non-photochemical quenching (A) and maximal quantum yield (B) in *H. akashiwo* (DIB), *H. akashiwo* (WA), and *C. subsalsa* (DIB). Error bars denote standard deviation (n = 3) and different letters represent significant difference within algae (One-way ANOVA, $p < 0.05$). 37

Figure 2.4 Scatter plots of σ_{PSII}' vs P_{Bmax} in *H. akashiwo* (DIB) (A), *H. akashiwo* (WA) (B), and *C. subsalsa* (DIB) (C). Data points include all temperature/CO_2 treatments: 25 °C + 375 ppm CO_2, 25 °C + 750 ppm CO_2, 30 °C + 375 ppm CO_2, and 30 °C + 750 ppm CO_2. Note: different scales used between panes for clarity in data presentation. 38

Figure 3.1 Maximum (closed circles) and effective (open circles) quantum yield of *H. akashiwo* grown on nitrate or ammonium with (+) or without (-) aeration. (*) and letters denote significant difference ($p < 0.05$) using one-way ANOVA (n = 4 ± S.D.) with Tukey's HSD post-hoc test..... 59

Figure 3.2 ETR_{max} of *H. akashiwo* grown on NO_3^- and NH_4^+ shifted from 60 to 785 µmoles quanta $m^{-2}s^{-1}$ at time zero. After 7 days (175 h) of semi-continuous growth, sodium tungstate (T) was added to cultures under high light (HL) and low light (LL) conditions. Error bars represent n = 4 ± S.D. 61

Figure 3.3 $F_v\backslash F_m$ of *H. akashiwo* grown on NO_3^- and NH_4^+ shifted from 60 to 785 µmoles quanta $m^{-2}s^{-1}$ at time zero. After 7 days (175 h) of semi-continuous growth, sodium tungstate (T) was added to cultures under high light (HL) and low light (LL) conditions. Error bars represent n = 4 ± S.D. 62

Figure 3.4 The ETR_{max} and ETR_{RCII} of *H. akashiwo* grown with either NO_3^- or NH_4^+ as the nitrogen source. Cultures were shifted from 60 to 785 µmoles quanta $m^{-2}s^{-1}$ at time zero and fluorescence was measured by (A) PAM fluorescence or (B) FIRe protocols. Sodium tungstate (T) was added to sub-cultures under high light (HL+T) and low light (LL+T) conditions and fluorescence was read four hours after the shift to high light. Error bar denote 1 ± S.D (n = 4). 64

Figure 3.5 Quantum yield (F_v/F_m) of *H. akashiwo* grown with either NO_3^- or NH_4^+ as the nitrogen source as measured by FIRe fluorometery. Cultures were shifted from 60 to 785 µmoles quanta $m^{-2}s^{-1}$ at time zero and fluorescence was measured over 24 hours. Sodium tungstate (T) was added to sub-cultures under high light (HL+T) and low light (LL+T) conditions and fluorescence was read four hours after the shift to high light. Error bars denote 1 ± S.D (n = 4). 65

Figure 3.6 The connectivity (ρ) of PSII of cells grown on NO_3^- or NH_4^+ as measured by FIRe fluorometery. Cultures were shifted from 60 to 785 µmol quanta m^{-2} s^{-1} at time zero. Sodium tungstate (T) was added to sub-cultures under high light (HL + T) and low light (LL + T) conditions and fluorescence was read four hours after the shift to high light Error bars denote n = 4 ± S.D. 66

Figure A.1 Spectral absorption for *H. akashiwo* (DIB) (A), *H. akashiwo* (WA) (B), and *C. subsalsa* (DIB) (C) under the four temperature and CO_2 treatments. Lines represent averages of four replicates. 75

Figure A.2 Light acclimated measurements of PSII maximal efficiency (A), functional absorption cross section (B), connectivity (C), and the rate of PSII reoxidation (D) in *H. akashiwo* (DIB), *H. akashiwo* (WA), and *C. subsalsa* (DIB). Error bars denote standard deviation (n = 3) and different letters represent significant difference within algae (One-way ANOVA, $p < 0.05$). Note: Fv'/Fm' and σ_{PSII}' were analyzed with FIRePro and ρ' and τ' were analyzed with FIReWorx 76

Figure A.3 Chlorophyll *a* based carbon assimilation of *H. akashiwo* (DIB) grown under 25 °C and bubbled with ambient air (375 ppm CO_2) or high CO_2 (750ppm CO_2). LB = low biomass, HB = high biomass, and LT = long term experiment. 77

ABSTRACT

During the past three decades the frequency and duration of harmful algal blooms (HABs) have significantly increased causing major economical losses world wide as well as being identified as the cause of a number of human health illnesses. These impacts have brought harmful algal species to the forefront of research efforts which are focused primarily on the effects of abiotic and biotic factors on algal growth. Less effort has been placed on understanding how changes in environmental parameters may impact harmful algal physiology. The effects of elevated CO_2 and temperature were studied using the raphidophytes *Chattonella subsalsa* and *Heterosigma akashiwo* isolated from the Delaware Inland Bays (DIB), and a cold water isolate of *H. akashiwo* from Puget Sound, WA. Neither increases in temperature, CO_2, or a combined treatment of elevated temperature and CO_2, had any significant effect on the growth rates of all three isolates. However, significant changes in physiology and carbon uptake were seen among temperature/CO_2 treatments and between strains. Both isolates of *H. akashiwo* exhibited changes in light harvesting capabilities in response to temperature, with a decrease in maximum carbon assimilation occurring in the cold water isolate. In contrast both elevated temperature and CO_2 altered the physiology of *C. subsalsa* although changes were not additive. Carbon assimilation increased in response to elevated CO_2 while temperature had a greater effect on light harvesting in this species. While growth and cell size did not change across any treatments in these raphidophytes, the large draw down of pCO_2

measured suggests that they could possibly be storing carbon, or releasing it as dissolved organic carbon. Thus, while the bloom dynamics of these HAB species will most likely not change with the predicted increases in global atmospheric carbon or temperature, a potential for them to alter phytoplankton community succession through changes in abiotic conditions remains a possibility.

The balance between light harvesting and carbon assimilation is a dynamic process in phytoplankton exposed to transient levels of light, temperature, and nutrients. When there is an imbalance in the delivery of excitation energy (i.e. photons of light) and carbon assimilation, phytoplankton are susceptible to damage to the photosynthetic electron transport chain. Thus, algae have evolved a number of mechanisms to dissipate excess electron energy during these periods of imbalance. The use of the nitrate reductase (NR) pathway as an electron sink during periods of saturating light was investigated in the DIB *H. akashiwo* strain. Electron transport through photosystem II and the impact of shifting this alga from low to high light was assessed with and without the addition of sodium tungstate, a NR inhibitor. Preliminary evidence suggests that this pathway is most likely only used as a short-term photoprotective mechanism. Further studies using simultaneous measurements of oxygen evolution or carbon assimilation and NR activity assays are suggested in order to more accurately state the possible contribution of this pathway as an electron sink.

Chapter 1

INTRODUCTION

Algae are critically important to marine and freshwater ecosystems. They are credited with over half of all the photosynthetic activity on earth and form the foundation of the numerous complex food webs from freshwater lakes to the open ocean (Rost et al. 2008). These small organisms are also largely responsible for driving important global biogeochemical cycles and especially for the export carbon from the atmosphere to deep waters by photosynthetic carbon fixation and sinking of organic matter (Falkowski et al. 2000).

However a number of both marine and freshwater phytoplankton have the ability to multiply quickly into intense blooms causing numerous detrimental consequences to surrounding ecosystems. For example the rapid increase in biomass of some harmful algal bloom (HAB) species can cause increased attenuation of light in the upper water column. The reduced light levels reaching the lower water column and benthic environments are capable of shading, thus killing, co-existing fauna such as sea grass and anchored macroalgae (Kemp et al. 2005). In addition to this, the inevitable collapse of blooms, when nutrients are exhausted, result in increased bacterial respiration rates. The large draw down in oxygen can result in anoxic conditions in the surrounding water column creating stressful or fatal conditions for any sedentary organisms. Some blooms, such as diatoms, directly affect fish due entirely to their physical structure. These silica encased cells with their sharp spines

irritate fish gills causing inflammation and subsequent mucus production leading to death due to asphyxiation (Yang and Albright 1992) .

Several species of harmful algal blooms (HABs) have also been shown to produce toxins such as domoic acid, brevetoxins, and paralytic shellfish poisons. Toxins produced by HABs can either be directly released into the water column, poisoning any organism that consumes it, or the toxic phytoplankton themselves can be consumed by fish or shellfish. Humans have also been adversely affected by these poisonous algae due to infected seafood consumption with close to 2,000 cases a year reported worldwide (Hallegraeff 2003). Various types of poisoning include paralytic shellfish poisoning (PSP), diarrhetic shellfish poisoning (DSP), amnesic shellfish poisoning (ASP), neurotoxic shellfish poisoning (NSP), and Ciguatera fish poisoning. Symptoms include, but are not limited to, abdominal pain, fever, respiratory paralysis, and in some cases death (HARRNESS 2005).

HABs not only adversely affect our health but also have huge impacts on our marine dependent economy and industries. Farmed fish are particularly at risk to HABs as they have no means of escape from blooms unlike their wild counter parts. Mariculture is practiced world wide and the massive mortality that occurs during blooms can result in substantial monetary losses. In the United States alone it was estimated that roughly $50 million per year was lost between 1987 and 1992 due to HABs (Anderson et al. 2000). HABs also result in fisheries and beach closures diminishing the recreational tourism that many communities depend upon. Beaching of deceased marine mammals and fish require removal and demand extra work hours of public health employees to issue alerts and organize the disposal of carcasses. In all, HABs can be accredited with numerous negative effects including massive fish,

shellfish, and marine mammal deaths, amnesic or neurotoxic shellfish poisoning, death of submerged aquatic vegetation, gastro-intestinal illness and even respiratory paralysis in humans, and a number of societal and economical impacts resulting in unquantified monetary losses (Anderson 1989).

Until several decades ago, HABs appeared to be an infrequent and rare occurrence, but now almost every coastal community world wide has been affected in one way or another by a toxic or harmful algal species. The increase in affected area, as well as higher losses to fisheries and tourism industries, have brought these phenomenon to the forefront of our management concerns (HARRNESS 2005). Several factors have been attributed with the marked increase in these blooms. It has been suggested that the larger number of observers and the increase in general community awareness has led to the rise in recorded blooms (Hallegraeff 1993). However, higher nutrient levels due to increases in coastal populations, aquaculture, and observed anthropogenic climate changes, have also been attributed with influencing blooms. In an effort to understand HABs, and even predict their occurrences, researchers have begun to conduct studies looking at the abiotic and biotic factors impacting the dynamics of bloom events. The effects of varying light, temperature, nutrient source, and CO_2 concentrations on microalgae have been studied individually or in concert. However, not much work has been done with multifactorial experiments where more than one interaction is measured. In light of the rapidly increasing effects of global climate change, these types of studies are essential to predicting long-term effects on HABs.

1.1 Light

Microalgae reside in extremely variable environments, especially when it comes to light. These microscopic organisms are largely at the mercy of the currents, waves, and tides which can expose phytoplankton to temporal changes in irradiance and intensity fluctuations of light. In response to these fluxes they have developed a number of internal mechanisms that affect light harvesting and photosynthetic capacity. Just like their terrestrial relatives, algae make use of photosynthetic pigments, including chlorophyll, organized within light harvesting protein complexes (LHCs) to gather photons. The number and size of LHCs is malleable and is influenced by the light level the algae resides within (Anning et al. 2000). During subsaturating conditions, cells increase chlorophyll *a* and photosynthetic unit levels to increase light absorption and efficiency. In contrast, exposure to high light increases cell division rate, and decreases chl *a*. This has been shown to be a universal response among most microalgae including diatoms (*Thalassiosira weisflogii*, Post et al. 1984; *Skeletonema costatum*, Anning et al. 2000), prymnesiophytes (*Emiliania huxleyi*, Harris et al. 2005), raphidophytes (*Heterosigma akashiwo*, Gao et al. 2007), dinoflagellates, and cryptophytes (*Karlodinium micrum* and *Storeatula major* respectively, Adolf et al. 2003). However, increased irradiance is not always beneficial to phytoplankton as the rise in photon flux can result in the over saturation of the electron transport chain thus creating free oxygen radicals (Apel and Hirt 2004). The formation of these hazardous molecules is reduced by using a number of different, but not mutually exclusive, systems described below. Despite these mechanisms, under prolonged exposure to high irradiance, the rate of photosynthetic unit damage can exceed the ability for repair causing a decrease in the photosynthetic capacity and

eventually result in photoinactivation of the cell (Jones and Kok 1966; Chow et al. 2005).

An important mechanism for protection during high light is the decrease of cells' absorption cross section, or the capacity for the cell to absorb light that is used for carbon fixation via the conventional photosynthetic electron transport chain (i.e. z-scheme). On shorter time scales phytoplankton will up regulate xanthophyll pigments, which have the unique ability to quench absorbed energy in the LHC before it can be passed on to the reaction center, thus preventing oxidative damage to the cell (Demmig-Adams 1990; MacIntyre et al. 2000; Falkowski and Raven 2007). On longer time scales phytoplankton can decrease the number or size of photosynthetic units (PSUs) as well as chl *a*, either by down regulation of the LHC pigments or due to increases in the division rate (Anning et al. 2000; Harris et al. 2005; Falkowski and Raven 2007). Several alternative mechanisms for dealing with changes in light have also been presented in raphidophytes. Warner & Madden (2007) suggested that despite the down-regulation of the number of functional PSII reaction centers during elevated irradiance, *Chattonella subsalsa* was able to maintain photosynthesis by lowering the electron transport rate, thus avoiding any photoinhibitory effects. Raphidophytes also utilize vertical migration as a method to avoid photodamage. Handy et al (2005) found that mixed raphidophyte blooms from the Delaware Inland Bays (DIBs) vertically migrate, rising to the top of the water column during light hours and settling on the bottom during dark hours. Interestingly, they found that *Heterosigma akashiwo* seemed to have the ability to sense and react to the light, staying at the bottom of the water column during continuous light experiments, while *C. subsalsa* continued to migrate on a light:dark cycle despite the constant irradiance.

In conclusion, all of the mentioned mechanisms allow the cell to continue photosynthesis while either protecting itself during high light conditions or efficiently capturing light during low light conditions.

1.2 Temperature

Along with fluxes in light, changes in temperature also govern the acclimation processes phytoplankton employ to survive. It is well known that temperature plays a crucial role in the function and survival of organisms and that by residing in, or maintaining, an optimal temperature they can ensure efficient metabolism and growth. Since algae can not control what temperature they inhabit, nor maintain an internal temperature on their own, they utilize a number of methods to achieve balanced growth. Processes dependent upon enzyme catalysts are primarily affected by shifts in temperature. As the light reactions of photosynthesis are independent of enzymes it could be thought that these steps will be unaffected by any temperature shifts in the surrounding environment. However, the rate of transfer of electrons through the thylakoid membrane, as well as the diffusion of associated molecules, will be hindered by membrane rigidity due to low temperatures or conversely increased membrane fluidity due to high temperatures (Raven and Geider 1988). Studies have shown that in many phytoplankton the physiological changes due to temperature are comparable to that of photoacclimation (Maxwell et al. 1994). For example, Anning et al (2001) demonstrated increased rates of photosynthesis, growth, and light harvesting pigment abundance in *Chaetoceros calcitrans* when switched to higher temperatures.

The Calvin-Benson cycle, dubbed the ‘dark reactions’, is reliant on enzymatic activity that is clearly temperature dependent. Due to this dependence, the

dark reactions will represent the rate limiting step of photosynthesis during low temperature conditions (Falkowski and Raven 2007). For example, Anning et al. (2001) showed significant decreases in light saturated photosynthetic rates (P_{Bmax}) when *C. calcitrans* was switched from 25 °C to 15 °C, and again from 15 °C to 6 °C, which was attributed to a decrease in activity of the enzyme Rubisco. In contrast, the effects of temperatures above the thermal optimum of photosynthesis on Rubisco activity have mainly been studied in vascular plants. For instance, studies in rice, soybean, and cotton plants all show a decrease in photosynthesis due to heat stress and subsequent decreases in Rubisco activity (Vu et al. 1997; Salvucci and Crafts-Brandner 2004). Such a imbalance in light harvesting and carbon fixation can eventually lead to an increase in excitation pressure at photosystem II; thus, exposure to temperatures below or above the growth optimum can lead to similar protective cellular processes utilized during exposure to high light. For example Maxwell et al (1994) found lower chlorophyll *a* $cell^{-1}$ and higher xanthophyll content in *Chlorella vulgaris* cells acclimated to 5 °C as opposed to cells grown at 27 °C. Again, these mechanisms are all used in an effort to protect the cell while still optimizing photosynthesis in response to external conditions.

1.3 Nutrients

Another major factor influencing algal blooms is the availability and assimilation of nutrients. As stated above, many coastal communities are experiencing high nutrient levels, in particular from urban and agricultural sources. Nitrate is considered a limiting macronutrient essential to phytoplankton; however nitrogen can be utilized in a number of forms and is considered to be one of the central factors in determining competitive outcomes among algal species (Tilman 1977). For example,

Zhang et al (2006) found that *Chattonella subsalsa* required almost double concentrations of nitrate and ammonium for growth when compared to *H. akashiwo*. However, reflecting on the earlier statement of the importance of multifactorial experiments, we must examine more than just the availability of nutrients when considering the dominance of one species over another.

Uptake and assimilation of nitrogen are internally regulated by light levels as well as temperature (Lomas and Glibert 1999; Parker and Armbrust 2005). Ammonium, being the most reduced form, can be directly used within the cell through a number of pathways leading to amino acid synthesis. Nitrate must first be reduced by nitrate reductase (NR), utilizing NAD(P)H, to nitrite and then further reduced by nitrite reductase (NiR), using ferredoxin, to ammonium (Lomas and Glibert 1999; Parker and Armbrust 2005). NAD(P)H and ferredoxin are both generated by the light reactions of photosynthesis which, as stated above, are highly dependent upon temperature and light conditions. Thus nitrogen assimilation not only depends on the immediate nutrient availability in the surrounding environment but also on the abiotic conditions. Other evidence suggests that nitrogen uptake is used not only for protein synthesis, but also as a sink for excess electrons generated by the light reactions of photosynthesis. Both Lomas & Gilbert (1999) and Parker & Ambrust (2005) worked with diatoms to show the effects of temperature on nitrogen uptake and assimilation. Lomas and Gilbert (1999) utilized diatom dominated bloom samples from the Chesapeake and Delaware bays. They provided evidence that these populations took up surplus NO_3^- and suggested that the reduction of this excess N pool could act as an electron bleed during periods of over saturation. Parker & Ambrust (2005) used molecular techniques to show the up-regulation of this electron sink pathway by

showing an increase in the mRNA encoding nitrate reductase during high light conditions in the diatom *Thalassiosira pseudonana*. The dissipation of excess energy by this pathway represents yet another acclimation method that photosynthetic cells can potentially use during periods of high excitation pressure on PSII.

1.4 Carbon

Lastly, the effects of atmospheric CO_2 levels should be considered when examining bloom events and dynamics. Over the past 200 years, human impact on global cycles, especially the burning of fossil fuels, has led to changes in climate, water cycles, and photosynthesis (Riebesell 2004). How these changes will alter microalgal growth and physiology depends primarily on how phytoplankton utilize carbon. Energy derived from light reactions is used to fix carbon through the Calvin-Benson Cycle using ribulose-1, 5-bisphosphate carboxylase-oxygenase (Rubisco) as its first catalytic enzyme. However, Rubisco has a higher affinity for oxygen, the substrate used in the photorespiration cycle, which leads to an alternative and more energetically expensive carbon fixation pathway. This predicament is partially overcome by compartmentalization of carbon fixation within the chloroplast. However, some algal groups have also developed further advantageous systems, called carbon concentrating mechanisms (CCMs), to increase CO_2 levels near the active site of Rubisco. These include the active transport of carbon dioxide or bicarbonate into the cell and the dehydration of HCO_3^- to CO_2 by the enzyme carbonic anhydrase (CA) internally or externally (Spalding et al. 2002). However, with global increases in CO_2, these mechanisms could become obsolete in the fight for dominance within algal communities. For example, The Intergovernmental Panel on Climate Change (IPCC 2007) have complied models that predict a temperature increase of 1.1 °C to 6.4 °C

and increases from current CO_2 concentrations of 375 ppm, to anywhere between 541 ppm to 970 ppm by the year 2100. Interestingly, no evidence has been found for the use of CA by the raphidophyte *H. akashiwo* as a CCM, indicating a potential competitive advantage of this alga in higher CO_2 conditions (Nimer et al. 1997).

Although it is debated whether phytoplankton are growth-limited by the current levels of atmospheric CO_2, studies have attributed elevated CO_2 levels with increased photosynthesis and growth in some species (Riebesell et al. 1993; Schippers et al. 2004). Furthermore, we know very little concerning the interactive or combined effects of changes in both CO_2 and temperature. For example, a study conducted by Fu et al. (2007) investigated the effects of increased CO_2 and temperature on two types of cyanobacteria. The four treatments were as follows: control (20 °C + 357 ppm), elevated CO_2 (20 °C + 750 ppm), increased temperature (24 °C + 375 ppm), and combined elevated CO_2 and temperature (24 °C + 750 ppm). In contrast to *Prochlorococcus*, significant increases in chl *a*-normalized photosynthesis in *Synechococcus* was noted when there were increases in CO_2 and temperature. Increases in the phycobiliproteins and associated pigments with these complexes in *Synechococcus* were seen during elevated temperature or CO_2 conditions alone or in combination, but the changes were not additive. However, the increase in the ratio of phycoerythrin to chl *a* occurred solely during enhanced temperature conditions leading them to suggest that chl *a* synthesis was more sensitive to temperature than CO_2 elevation in *Synechococcus*. In a latter experiment by Fu et al (2008), the photosynthetic parameters of the raphidophyte *H. akashiwo* and the dinoflagellate *Prorocentrum minimum* were compared when grown under the same four growth conditions of their previous study. CO_2 enrichment significantly increased the carbon

fixation rate in *P. minimum*, regardless of temperature, but only had an effect under elevated temperature in *H. akashiwo*. However, growth did not depart from control levels in *P. minimum* while *H. akashiwo* had roughly a 33% increase in growth across all three treatments in comparison to the control. The faster growth rates of *H. akashiwo*, in combination with a significant rise in photosynthetic efficiency (α) across all treatments, suggested a potential competitive advantage over *P. minimum*.

Gordillo et al. (2003) conducted a similar experiment using the chlorophyte *Dunaliella viridis* where the effects of increased CO_2 levels (ambient – 0.035% vs high CO_2 – 1%) were studied along with the added factor of nitrogen limitation (low nitrate – 0.5 mM vs high nitrate – 5 mM). A positive response of photosynthesis and growth under increased CO_2 levels and nitrogen sufficient conditions was observed, however they found that this response was not coupled with any changes in chlorophyll content nor LHC size. It was suggested that nitrogen sufficient cells reacted by increasing the number of PSII reactions centers, but reduced PSU size, when under higher CO_2 conditions, thus enhancing photosynthesis. When cultures were N-limited, the positive effects of CO_2 were not seen, and cells released dissolved organic carbon (DOC) as an alternative acclimative strategy to prevent oxidative stress in the cell. A pulse amplitude modulated fluorometer was used to measure variable fluorescence and estimate relative electron transport rate (rETR) from PSII to PSI. Higher rETR, calculated as $\Delta F/Fm' \times$ photon fluence rate (PFR), was found under the high CO_2 + low nitrate conditions which, in combination with the bleed of carbon out of the cell, allowed for the maintenance of the C:N ratio. It is evident that algae are complex organisms whose responses to varying abiotic conditions elicit numerous reactions depending upon the species. These studies all

give us clues as to how phytoplankton will react to increasing CO_2 levels in conjunction with changes in temperature or nitrogen. However it is vital to begin to study the combined effects of these conditions in order to be able to predict physiological differences in HAB species in light of projected climate change scenarios in the near future.

1.5 Model Species

Two common HAB species in the DIBs are the raphidophytes *H. akashiwo* and *C. subsalsa*. Structurally described as 'naked' these cells have no cell wall and are characterized as having two flagella, numerous golden-brown chloroplasts and the primary photosynthetic pigments chl *a* and fucoxanthin. Both species have been evident as harmful algae for a number of decades and continue to be the cause of massive fish kills and immeasurable losses in revenue in many parts of the world (Hallegraeff and Hara 2003). For example, in 2006 a single *H. akashiwo* bloom off of Puget Sound resulted in a 2 million dollar loss in revenue from local salmon farms and in 1972 a bloom of *Chattonella* in the Seto Island Sea of Japan decimated the yellow tail industry resulting in the loss of about 14,000,000 yellowtail worth over 7.1 billion ¥ (roughly 77.8 million in today's USD) (Okaichi 1989; Rensel 2007). Their blooms have been attributed to increased eutrophication in Japan, New Zealand, British Columbia, and on the west and east coast of the United States (Honjo 1991). Although wide spread, differences in geographical isolates of species have also been noted. *H. akashiwo* has been observed along the entire East Coast of the United States however, no fish kills have been positively linked to their blooms in the Atlantic basin. Interestingly, a study by Connell (2000) found the nuclear internal transcribed spacer (ITS) region of 18 isolates of *H. akashiwo* from distant localities in

the northern and southern hemisphere to be identical (98.31% similar by pairwise comparison), suggesting a more recent global distribution possibly aided by ship ballast water.

Despite their undisputed role as HAB species the exact toxicological mechanisms and environmental triggers of toxins in *H. akashiwo* and *C. subsalsa* are still debated. Recent studies show that raphidophyte blooms, including *Chattonella* sp. and *Heterosigma* sp., are able to generate large amounts of reactive oxygen species (ROS), which could be responsible for altering gill structure and function in fish (Oda et al. 1994; Oda et al. 1997; Kim et al. 2004). Twiner and Trick (2000) measured substantial amounts of hydrogen peroxide and concluded that this ROS was produced via an enzymatic process linked to a decrease in iron availability, confirming this phenomenon in *H. akashiwo*. However, in a more recent study it was shown that the H_2O_2 formed by *H. akashiwo* was orders of magnitude too low to induce any negative effects on invertebrate and vertebrate cell lines of *Artemia salina* (brine shrimp) (Twiner et al. 2001). It is suggested that raphidophytes are able to produce brevetoxins or brevetoxin-like compounds (Khan et al. 1997; Bourdelais et al. 2002; Keppler et al. 2006). Regardless of their toxicity mechanisms, these algae have solidified themselves as an immediate and lingering threat to fisheries in many parts of the world.

To date, many experiments have investigated the individual effects of temperature, nitrogen source, and CO_2 concentration on the growth rates and photobiology of a number of algae species. However, the combined effects of all three of these factors have yet to be thoroughly evaluated. Likewise, there has been a greater focus on open ocean phytoplankton species such as *Emiliania* and *Trichodesmium*. Taking into account the predicted increases in atmospheric CO_2, the

lack of evidence for the use of CA in *H. akashiwo* could allow for even more frequent and damaging blooms than we are currently experiencing (Nimer et al. 1997; IPCC 2007) . Being able to predict how algae will respond to these anthropogenic effects depends upon our knowledge of their key growth and physiological responses when exposed to changing temperature, CO_2 and nutrients. Not only will this information be economically valuable in terms of fisheries and their sustainability but it will also be important for the survival of the tourism industries that depend on beaches and coastal waterways. Thus the goal of my thesis was two fold: 1) to investigate the long-term impact of elevated CO_2 and temperature on three different isolates of raphidophyte and 2) to test for possible differences in photosynthetic electron transport when *H. akashiwo* is grown under two different sources of inorganic nitrogen.

Chapter 2

THE IMPACT OF LONG TERM SHIFTS IN CO_2 AND TEMPERATURE ON THE GROWTH AND PHYSIOLOGY OF *HETEROSIGMA AKASHIWO* AND *CHATTONELLA SUBSALSA*

ABSTRACT

Over the last three decades the increase in number and duration of harmful algal blooms (HABs) has garnered international attention. The environmental and economic losses associated with these blooms have led to the initiation of numerous studies investigating the triggers of HABs. In this study we utilize two isolates of the raphidophyte *Heterosigma akashiwo* originally collected from the Delaware Inland Bays (DIB) and Puget Sound and the sympatric DIB species *Chattonella subsalsa*. Lack of evidence for a carbon concentrating mechanism (CCM) in these species suggests the potential for increases in blooms with the predicted rises in temperature and CO_2 under a global climate change scenario (Nimer et al. 1997; IPCC 2007). Growth and physiology was evaluated after long-term acclimation to four different temperature and CO_2 treatments as follows: 'control' (25 °C + 375 ppm CO_2), 'high CO_2' (25 °C + 750 ppm CO_2), 'high temperature' (30 °C + 375ppm CO_2), and 'combined' (30 °C + 750 ppm CO_2). No changes in batch growth were found in any of the four conditions for all three isolates. However significant differences in light harvesting capabilities, photochemistry, and carbon assimilation were observed indicating distinct variations in physiology between species. *H. akashiwo* from the DIB did not exhibit any changes in carbon assimilation between treatments, but was

found to increase light harvesting capabilities and photosynthetic efficiency corresponding to a decrease in non-photochemical quenching (NPQ) under elevated temperatures. Likewise the Puget Sound isolate of *H. akashiwo* increased light harvesting and decreased NPQ at elevated temperatures, however there was no change in photosynthetic efficiency or maximal quantum yield, and so carbon fixation decreased at 30 °C. In contrast, *C. subsalsa* responded to both temperature and CO_2. The elevation of CO_2 increased carbon assimilation under both 25 °C and 30 °C, however under elevated temperatures the increase in excitation pressure caused a rise in NPQ with a decrease in light harvesting in order to maintain carbon fixation. It has long been known that phytoplankton can adjust their light harvesting capabilities on short time scales through a number of mechanisms in order to maintain balance between photon absorption and carbon fixation when subjected to rapid changes in their environment. Here we provide evidence for the long-term acclimation of raphidophytes to elevated temperature and CO_2 and suggest that despite their potential for enhanced growth, it is possible that the range of temperature/CO_2 levels used here are not enough to induce this change.

2.1 INTRODUCTION

Human industrial activity has increased atmospheric carbon dioxide (CO_2) from pre-industrial values of 280 ppm to 379 ppm in 2005, with an expected increase between 541 ppm to 970 ppm by the year 2100 (IPCC 2007). The oceans have been the primary sink of the anthropogenic CO_2, resulting from utilization of fossil fuels, and its absorption has measurably altered the carbonate chemistry system. As CO_2 dissolves into the surface seawater it reacts with H_2O to form carbonic acid (H_2CO_3) which dissociates into bicarbonate (HCO_3^-) and carbonate (CO_3^{2-}). Currently the sum

of these carbon compounds, collectively known as dissolved inorganic carbon (DIC), are primarily in the form of HCO_3^- and CO_3^{2-}. However, as atmospheric CO_2 continues to rise the total DIC pool will increase, with the equilibrium shifting to higher CO_2 and HCO_3^- while the CO_3^{2-} concentration will decrease with the coinciding drop in pH (Zeebe and Wolf-Gladrow 2001).

$$CO_2 + H_2O \leftrightarrow HCO_3^- + H^+ \leftrightarrow CO_3^{2-} + 2H^+$$

Precipitation of calcium carbonate also acts as a source of CO_2 to the water column, however with rising CO_2 and decreasing pH, the balance of the equation will be in favor of bicarbonate and not calcification.

$$Ca^{2+} + 2HCO_3^- \rightarrow CaCO_3 + CO_2 + H_2O$$

These changes are especially significant when considering marine calcifiers such as corals, coccolithophores, echinoderms, and mollusks. Two recent experiments have shown the link between rising CO_2 and decreases in calcification rates in a coral community and in the coccolithophore *Emiliania huxleyi*, with both studies showing a 40% decrease in calcification going from pre-industrial pCO_2 levels to predicted future pCO_2 levels (Langdon et al. 2000; Delille et al. 2005, respectively).

In contrast, it is generally thought that phototrophs are not limited by carbon due to the large DIC pool available in seawater. Despite this, the sensitivity of growth and photosynthesis to CO_2 enrichment or depletion has been shown in diatoms, chlorophytes, cyanobacteria, and raphidophytes (Riebesell et al. 1993; Gordillo et al. 2003; Fu et al. 2007; Fu et al. 2008). This has been attributed to the low affinity of the primary carboxylating enzyme Rubisco for CO_2. For example, Rost et al (2003) measured carbon acquisition in three species of bloom forming algae finding that *Phaeocystis globosa*, a flagellate, was close to saturation under present day CO_2

levels due to their highly efficient carbon concentration mechanisms (CCMs). In contrast, the cocccolithophore *E. huxleyi* had much higher half saturation constants for CO_2 across a range of CO_2 levels (36 to 1800 ppmv) in comparison with both *P. globosa* and the diatom *Skeletonema costatum* indicating a greater sensitivity to changes in CO_2. It has been suggested that increases in available atmospheric carbon could allow for increased photosynthesis and growth in phytoplankton lacking CCMs, thus reducing the competitive advantage of those alga utilizing CCMs and potentially altering the phytoplankton community (Raven 1991). However, depending on the underlying processes, the effects of rising CO_2 may be strongly influenced by temperature, light, and nutrient availability.

To date, several experimental designs have been utilized to study the effects of changing seawater carbon chemistry on phytoplankton and are organized into two basic approaches: altering the total alkalinity (TA) while maintaining a constant DIC, or by changing DIC with a constant TA (Hurd et al. 2009; Schulz et al. 2009). TA is most easily defined as the sum of carbonate alkalinity, borate alkalinity and water alkalinity (see Zeebe and Wolf-Gladrow 2001 for details). TA can be modified by the addition of strong acids, such as hydrochloric acid (HCl) to reduce the alkalinity or strong bases, such as sodium hydroxide (NaOH), to increase alkalinity. Experiments altering TA are done in gas-tight bottles and although the resulting change in pH will shift the equilibrium concentrations of the carbon species, the total DIC cannot change from release or invasion of CO_2. This design is well suited for those phytoplankton sensitive to continuous bubbling but does not present the most realistic simulation of ocean acidification (i.e. changing DIC at constant TA) (Riebesell et al. 2000; Rost et al. 2008; Schulz et al. 2009).

The second experimental approach adjusts DIC with a constant TA and can be achieved through a number of methods. The first is through the aeration of cultures with gas mixtures of different pCO_2. Like a natural open system, this adjusts aquatic partial pressure of CO_2 by allowing an equilibrium to establish between the head space of the culture and the seawater medium. Although this method allows for easy adjustment of pCO_2 levels, equilibrium can potentially take a long time and the physiological impact of bubbling to an organism must also be taken into account. The second method for altering DIC is through the injection of CO_2 free or enriched seawater. However, this method is most suitable only for large volume experiments as it takes about one liter of CO_2 enriched seawater per cubic meter to reduce pH by 0.2 units (Schulz et al. 2009). The last method of changing DIC at constant TA is through the addition of sodium bicarbonate ($NaHCO_3$) and sodium carbonate (Na_2CO_3), with HCl to buffer TA. This allows for the effects of CO_2, without changes in pH, to be examined. This method can be extremely precise, but is usually ideal only for small scale experiments (Delille et al. 2005; Rost et al. 2008; Shi et al. 2009).

Regardless of the approach used to alter the seawater pCO_2 it is important to take into account the effects of biological activity on the carbonate system. As photosynthesis increases, CO_2 and DIC will be consumed, shifting the system towards a higher pH. On the other hand when working with calcifying species $CaCO_3$ is precipitated from the water column, also decreasing the DIC, and more strongly the TA. Thus the equilibrium will shift to a lower pH and higher CO_2 concentrations. Depending on the ratio of photosynthesis to calcification, pCO_2 concentrations will rise, stay steady, or decline. When working with high cell densities the biological draw down of CO_2 can quickly exceed the supply rate causing shifts in the

experimental carbon chemistry (Hurd et al. 2009). For example, in a mesocosm experiment titled Pelagic Ecosystem CO_2 Enrichment study III (PeECE III), reported by Riebesell et al (2007), Schulz et al (2008), and Egge et al (2009), the development and decline of nutrient induced algal blooms were followed for a period of 24 days. Natural plankton communities were enclosed in $27m^3$ polyethylene bags and initially aerated to target CO_2 levels of ~350 µatm, 700 µatm, and 1050 µatm. They found the rate of inorganic carbon consumption to be significantly higher for those mesocosms exposed to higher pCO_2 with all mesocosms decreasing to ~ 200, 350, and 460 µatm, respectively. Hence, when working with bloom levels of phytoplankton this added factor of biological draw down must be taken into account when considering experimental design.

In a global climate change scenario, temperature is expected to rise anywhere from 1.1 to 6 °C by 2100. In contrast to increases in CO_2, increased temperature does not always result in faster growth or the up-regulation of cellular processes. It is well established that distinct phytoplankton groups have optimal temperature for growth and exhibit a bell shaped curve with peak metabolic rates occurring over the optimal temperature range (Falkowski and Raven 2007). Thus, the proposed scenarios of increasing sea surface temperatures and CO_2 over the next 100 years could hinder or enhance growth and photosynthesis depending upon algal type. To date numerous researchers have examined the effects of changing temperature and pCO_2 on phytoplankton both individually and in concert (Riebesell et al. 1993; Anning et al. 2001; Riebesell 2004; Burns et al. 2005; Delille et al. 2005; Fu et al. 2007; Feng et al. 2008; Fu et al. 2008). Phytoplankton responses to increasing CO_2 have been found to vary with coinciding increases in temperature, even at the species

level. For example increased rates in growth and photosynthesis were noted in *H. akashiwo*, *E. huxleyi*, and *Synechococcus* but not in *P. minimum* or *Synechococcus* (Burns et al. 2005; Fu et al. 2007; Feng et al. 2008; Fu et al. 2008). However these studies only considered the effects of short-term increases in these two parameters (10 – 15 days) while the effects of long-term shifts are largely unknown.

The changes in ocean carbon chemistry and temperature over the next century could have profound effects not only at the species level, but on the phytoplankton community and ocean ecosystems as a whole. Fluctuations in competition and succession can play a large role in the health and robustness of ecosystems, especially in the context of Harmful Algal Blooms (HABs). HABs are simply defined as blooms of phytoplankton that can produce harmful or toxic effects to humans, fish, shellfish, plants, animals, and birds. Over the past three decades increases in the number and duration of HAB events have initiated investigations into physiology of HAB species and the dynamics of their blooms. Our approach here was to investigate the effects of long term acclimation to temperature and CO_2 addition on three HAB species belonging to the class raphidophyceae. Two strains of *Heterosigma akashiwo*, originating from the Delaware Inland Bays (DIB) and the Puget Sound, and *Chattonella subsalsa*, also from the DIB, were first acclimated to 25 °C and 30 °C and bubbled with both ambient air, 375 ppm CO_2, and a CO_2 mixture of 750 ppm for 21 days. After the acclimation period, cell biomass was held at bloom concentrations, between 400 and 800 ug chl *a* L^{-1}, by semi-continuous dilutions for 10 days. Like the PeCEC III mesocosm experiment, our aim was to examine the effects of elevated CO_2, in combination with temperature, on the physiology and growth of phytoplankton during bloom conditions (Riebesell et al. 2007; Schulz et al. 2008; Egge et al. 2009).

2.2 METHODS AND MATERIALS

2.2.1 Isolates and culture conditions

All three strains used in this work are available from the Provasoli-Guillard Center for the Culture of Marine Phytoplankton (https://ccmp.bigelow.org/home) (CCMP). *Heterosigma akashiwo* (CCMP 2393) and *Chattonella subsalsa* (CCMP 2191) were originally isolated by Y. Zhang and K. Coyne from Torquay Canal, Rehoboth Bay and Love Creek, Rehoboth Bay, DE, USA respectively, between 2001 and 2002. *H. akashiwo* (CCMP 2808) was originally isolated by S. Strom from Guemes Channel, Puget Sound, WA, USA in June of 2006. Stock cultures were maintained on modified f/2 media from offshore seawater that was diluted to a salinity of 26 ‰ with Mill-Q water, before the addition of nutrients and trace metals. Final concentrations of $NaNO_3$ and NaH_2PO_4 were 150 µM and 6.165 µM respectively. Stock cultures were grown at 25 °C and 30 °C in order to simulate peak summertime temperatures in DIB and the expected increase of ~ 5 °C by the year 2100 (Zhang et al. 2006; IPCC 2007), and grown at an irradiance of ~185 µmol quanta $m^{-2}s^{-1}$ provided by cool white fluorescent lamps set to a 12:12 h light dark cycle.

2.2.2 Experimental design

Experiments were preformed in 500 ml glass Erlenmeyer flasks with a silicone stopper retrofitted with borosilicate inlet and outlet glass rods. The inlet opening had a 0.2 micron filter attached with a piece of silicone tubing while the outlet opening was plugged with cotton. Cultures were initially maintained in batch growth and bubbled with ambient air for 7 days prior to the start of each experiment to counteract any inhibitory effects of physical stress due to the increased turbulence

from bubbling. Replicate (n=4) cultures were grown at each of the following four conditions: 'control': 25 °C and present day CO_2 (375 ppm); 'high CO_2': 25 °C with high CO_2 (750 ppm); 'high temperature': 30 °C and present day CO_2 (375 ppm); 'combined': 30 °C with high CO_2 (750 ppm). CO_2 concentrations were obtained by gently bubbling cultures with a premixed compressed air/CO_2 mixture (Scott Gas) and fresh media was also adjusted to temperature and CO_2 conditions prior to its use in any cultures. Prior to semi-continuous culturing, cultures were held in 3 batch-growth cycles, lasting 7 days each, with a 95% media exchange at the start of each batch interval, to keep the cells in log-phase growth. Final sampling was conducted after 10 days of semi-continuous growth.

2.2.3 Growth rates, chlorophyll *a*, and fluorescence measurements

Cell counts were taken every day using a Beckman Multisizer 3 Coulter Counter were initially verified for accuracy with light microscopy. Growth rates were calculated during the third week of batch growth under experimental conditions using the equation:

$$\mu = \frac{\ln(N_2 / N_1)}{t_2 - t_1}$$

where N_1 and N_2 are the average values of cell numbers at times t_1 and t_2 spanning the linear portion of the growth curve over 3 or 4 days. During semi-continuous growth, cell counts, chlorophyll *a* (Chl *a*), and chlorophyll fluorescence measurements were taken every other day before dilution in order to monitor cultures for steady state growth conditions. Steady state was defined as no significant change in these parameters over 10 days.

Chl *a* was measured by filtering duplicate subsamples from each replicate flask onto GF/A glass fiber filters, followed by extraction in 5 ml of 90% acetone for 24 h at -20 °C before reading on a Turner 10-AU fluorometer. Chlorophyll *a* fluorescence of intact cells was conducted on 1 ml subsamples from each flask and read on a Fluorescence Induction and Relaxation fluorometer (FIRe, Satlantic) between hours 2 and 3 of the light cycle. Single turnover fluorescence was measured by applying a 100 μs flash of blue light (450 nm), followed by a series of flashes over 500 ms to record the reoxidation of the Q_A quinone in PSII. After this relaxation period multiple turnover fluorescence was measured by applying a long pulse of light for 20 ms in order to saturate the PSII and PQ pool. The protocol ended by applying a weak light for one second to measure the subsequent reoxidation of the PQ pool. The difference between the steady state fluorescence (F_o), and maximal fluorescence (F_m) read during the first induction step in the dark, was used to calculate the variable fluorescence (F_v). F_v/F_m, or the maximum quantum yield of PSII, is an indication of PSII efficiency (Butler 1978; Baker 2008). Sigma (σ), the functional absorption cross section of PSII, connectivity (ρ), a dimensionless parameter defining the energy transfer between PSII units, and tau (τ), the time constant for reoxidation of the PSII reaction center Q_A quinone, were also measured using the FIRe system. PSII photochemistry parameters were determined by fitting the four step fluorescence trace using the FIRePRO software provided by Satlantic Inc and open source software Fireworx version 0.9.1.

H. akashiwo and *C. subsalsa* were subjected to different dark adaptation protocols prior to measuring fluorescence in the FIRe. Pilot tests conducted by myself and Sebastian Hennige showed a significant decrease in F_v/F_m in *H. akashiwo* when

cells were dark acclimated for longer than 5 minutes. This was most likely due to a dark reduction of the PQ pool and PSII due to a chlororespiratory pathway present in *H. akashiwo*, similar to that noted in diatoms and chlorophytes (Dijkman and Kroon 2002; Peltier and Cournac 2002). Therefore *H. akashiwo* was held under low light conditions and dark adapted for 2 minutes, while *C. subsalsa* was dark-adapted for 20 minutes, prior to taking fluorescence readings.

Final day sampling differed slightly from the semi-continuous protocol. Chl *a* samples were taken in triplicate and FIRe readings were also conducted in the light adapted states as well as in the dark. After measuring fluorescence under dark adapted conditions samples were exposed to 5 minutes of growth light (~185 μmol quanta $m^{-2}s^{-1}$) using the separate actinic light source provided by a blue LED array before measuring the maximal fluorescence, PSII absorption cross section and PSII efficiency in the light adapted state (F_m', σ_{PSII}', F_v/F_m'). Antenna based non-photochemical quenching (NPQ) was calculated as in Suggett et al (2008) follows:

$$NPQ = 1 - (\sigma'_{PSII} / \sigma_{PSII})$$

2.2.4 Determination of P:E curves, primary production, and light absorption

To evaluate the response of each strain to rising temperature and CO_2 conditions, ^{14}C photosynthesis to irradiance (P:E) curves were conducted along with standard 24 h primary production measurements. P:E curves were preformed by measuring carbon fixation rates over a short period of time, while primary production measurements were used to calculate the daily carbon production rates of each strain. 1 milliliter subsamples were spiked with 0.1 μCi ml^{-1} ^{14}C sodium bicarbonate (MP Biomedicals) and incubated at varying light intensities (10 to 1000 μmol photons $m^{-2}s^{-1}$) for 30 minutes using a photosynthetron (CHPT Inc.) set to the growth temperature.

Two samples from each set were wrapped in tinfoil to estimate dark fixation and total added activity was measured from three 100 µl aliquots of spiked samples added to 5 ml of Ultima Gold Cocktail (PerkinElmer) solution containing 200 µl of phenylethylamine. After the 30 minute incubation period, samples were fixed with 10% gluteraldehyde and acidified with 250 µl of 6N HCL. One subsample from each set was also fixed and acidified prior to the 30 minute incubation in order to estimate any background radiation. Samples were then gently shaken overnight in the hood in order for any excess sodium bicarbonate to evaporate. 5 ml of cocktail solution was added to each sample before reading on a Wallac System 1400 liquid scintillation counter. ^{14}C uptake rates were corrected for any dark uptake before being normalized to Chl *a* and P-E curves were fitted using the exponential function of Platt et al.(1980). From this empirical equation the maximum chlorophyll specific carbon fixation rate P_{Bmax} [µg C µg Chl a^{-1} h^{-1}], and α^B, the initial slope of the P:E curve, [µg C (µg Chl *a*)$^{-1}$ h^{-1} (µmol quanta $m^{-2}s^{-1}$)$^{-1}$] were calculated. E_k, defined as the saturation irradiance point, was calculated from P_{Bmax}/ α^B (Fu et al. 2008).

Primary production rates were measured by spiking two 15 ml subsamples from each flask with 0.033 µCi ^{14}C ml^{-1}. Total activity was estimated by taking 100 µl aliquots from spiked samples and adding it to a vial containing 5 mL of Optiphase 'HiSafe 3'cocktail solution (PerkinElmer) plus 200 µl of phenylethylamine. Of the two spiked samples, one sample was placed back into the incubator for 24 hours before being filtered while the second was immediately filtered onto a GF/F filter and used as a background blank. Filters were added to 5 mL of cocktail solution before reading on a Wallac System 1400 liquid scintillation counter.

The absorption spectra of each sample was measured on a spectrophotometer fitted with an integrating sphere (Shimadzu UV-2401). Cells were either first concentrated onto GF/F filters (*H. akashiwo* 2393) or measured in solution (*H. akashiwo* 2808 & *C. subsalsa* 2191). Absorption spectra were corrected for differential scattering at each wavelength by subtracting the average optical density measured between 740 nm (filters) or 730 nm (in vivo) and 750 nm. The corrected optical densities were then used to calculate absorption coefficients, a*, normalized to Chl *a* using previously determined β correction factors as in Cleveland and Weidemann (1993). Once normalized, the average (400 -700 nm) Chl *a* specific a* was calculated. The maximal quantum yield of photosynthesis, Φ_{max}, under each treatment was calculated from the ratio of α^B to a*, corrected for the spectra of the photosynthetron, and converted to moles of carbon per moles of light.

Table 2.1 Chlorophyll fluorescence parameters as measured by Fluorescence Induction and Relaxation (FIRe) fluorometery.

Symbol	Parameter	Definition
F_o or F_o'	Minimum fluorescence	Fluorescence emission from dark or light adapted cells – level of emission when Q_A is fully oxidized
F_m or F_m'	Maximal fluorescence	Maximum fluorescence emission – level of emission when Q_A is fully reduced by PSII
F_v/F_m or F_v/F_m'	Quantum yield	Maximum efficiency at which light absorbed by PSII is used for reduction of Q_A
σ_{PSII} or σ'_{PSII}	Absorption cross-section	Probability of excitation from LHC being used for a photochemical reaction
ρ or ρ'	Connectivity	The probability that an excitation which encounters a reaction center in the open state will be transferred to a neighboring reaction center.
τ or τ'	Tau	The time constant for reoxidation of the PSII reaction center Q_A quinine
NPQ	Non-photochemical quenching	Chl *a* based energy dissipation from the light LHC calculated as: $1 - (\sigma'_{PSII}/ \sigma_{PSII})$

Symbols followed by ' are measured in the light adapted state after exposure for five minutes to an actinic light provided by a blue LED array set to growth irradiance (~ 185 µmol quanta m^{-2} s^{-1}).

2.2.5 pH, dissolved inorganic carbon and partial pressure of CO_2

Samples for pH and dissolved inorganic carbon (DIC) analysis were collected on the final sampling day just prior to the start of the light cycle. pH samples were analyzed using a Fisher Scientific AR15 Accumet Research pH meter. 22 ml aliquots were collected for DIC samples in glass vials fitted with conical caps and immediately preserved with 200 µl of 5% $HgCl_2$ before being stored at 4 °C. Total DIC was determined within one week of sampling using an acid sparging instrument built by J.H. Sharp's lab and modeled after the Monterey Bay Aquarium Research Institute AMICA system developed by G.E. Friederich. Samples, 1.25 ml, were injected into a gas stripping column containing 0.1 ml of 5% phosphoric acid solution effectively acidifying the DIC pool and converting it into dissolved CO_2. Constant nitrogen flow into the cell was used to strip the sample of CO_2, which was then passed through a drying magnesium perchlorate column and subsequently analyzed by an infrared analyzer with high precision flow control (Li-cor Biosciences, Lincoln, NE, USA; Friederich et al. 2002). Partial pressure of CO_2 was calculated from DIC and pH using the CO2SYS package version 01.05 written by Ernie Lewis (Table A.1). Calculations were preformed using the GEOSECS (Li et al. 1969) option for acidity constants, the borate acidity constant of Dickson (1990), and the seawater pH scale.

2.2.6 Statistics

Growth rates and photosynthetic parameters for all experiments were compared using a one-way ANOVA, unless otherwise noted, followed by Tukey HSD post hoc testing using SPSS (Version 16.0). Data were assessed for normality and

homoscedasticity and when necessary were log transformed prior to any statistical analysis. In the event that transformation did not help with distribution or variance, data were evaluated using the non-parametric Kruskal-Wallis test and the Mann-Whitney U post hoc test. Differences were deemed significant when $p < 0.05$. Correlation between P_{Bmax} and σ_{PSII}' was assessed using the Pearson product-moment correlation coefficient and deemed significant when $p < 0.05$.

2.3 RESULTS

2.3.1 Growth and carbon assimilation

Growth rates did not differ between treatments for any of the three raphidophytes tested (Fig. 2.1A), however significant differences in response to elevated temperature and CO_2 were seen in the light harvesting capabilities and carbon assimilation. Carbon assimilation in the DIB strain of *H. akashiwo* showed a slight, although insignificant, increase to elevated temperature and the combined treatment (Fig. 2.1B). A similar trend was noted for 24 h primary productivity measurements, with no significant differences between treatments (Fig. 2.1D). However, photosynthetic efficiency (α) increased significantly under the higher growth temperature with no apparent effects of CO_2 addition (Fig. 2.1C, Table A.2). In contrast, short and long-term maximal photosynthesis in *H. akashiwo* originally collected from Puget Sound was negatively impacted by elevated temperature and resulted in a significant drop in P_{Bmax}, when compared to the control treatment (Fig. 2.1B and D, Table A.2). However, the addition of CO_2 combined with elevated temperature appeared to alleviate this loss in productivity as P_{Bmax} was significantly higher than the elevated temperature treatment alone (Fig. 2.1B). There was no

significant change in α in the Washington *H. akashiwo* isolate between any treatment conditions (Fig. 2.1C, Table A.2).

In contrast to the two strains of *H. akashiwo*, carbon assimilation in *Chattonella subsalsa* showed a greater response to CO_2 addition with minimal effect of temperature. Both short-term, P_{Bmax}, and long-term, primary productivity, exhibited a significant increase in the presence of higher CO_2 but little to no change with the rise in temperature (Fig. 2.1 B and D, Table A.2). Photosynthetic efficiency was significantly higher in the elevated CO_2, the elevated temperature, and in the combined treatment relative to the control, however there was no difference in α between the three different treatments (Fig. 2.1 C, Table A.2).

Interspecific comparison revealed significant differences in maximal photosynthesis only under the control conditions of 25 °C and ambient air with the Puget Sound *H. akashiwo* maintaining a greater P_{Bmax} value than the DIB *H. akashiwo* and *C. subsalsa* (Fig. 2.1A, Table A.3). However, primary productivity rates were significantly higher in *C. subsalsa* across all treatments and photosynthetic efficiency of the Puget Sound *H. akashiwo* was significantly lower compared to the DIB isolate and *C. subsalsa* (Fig. 2.1 C and D). DIB *H. akashiwo* exhibited significantly greater growth rates than both the Washington *H. akashiwo* strain and *C. subsalsa* (Fig. 2.1A, Table A.3).

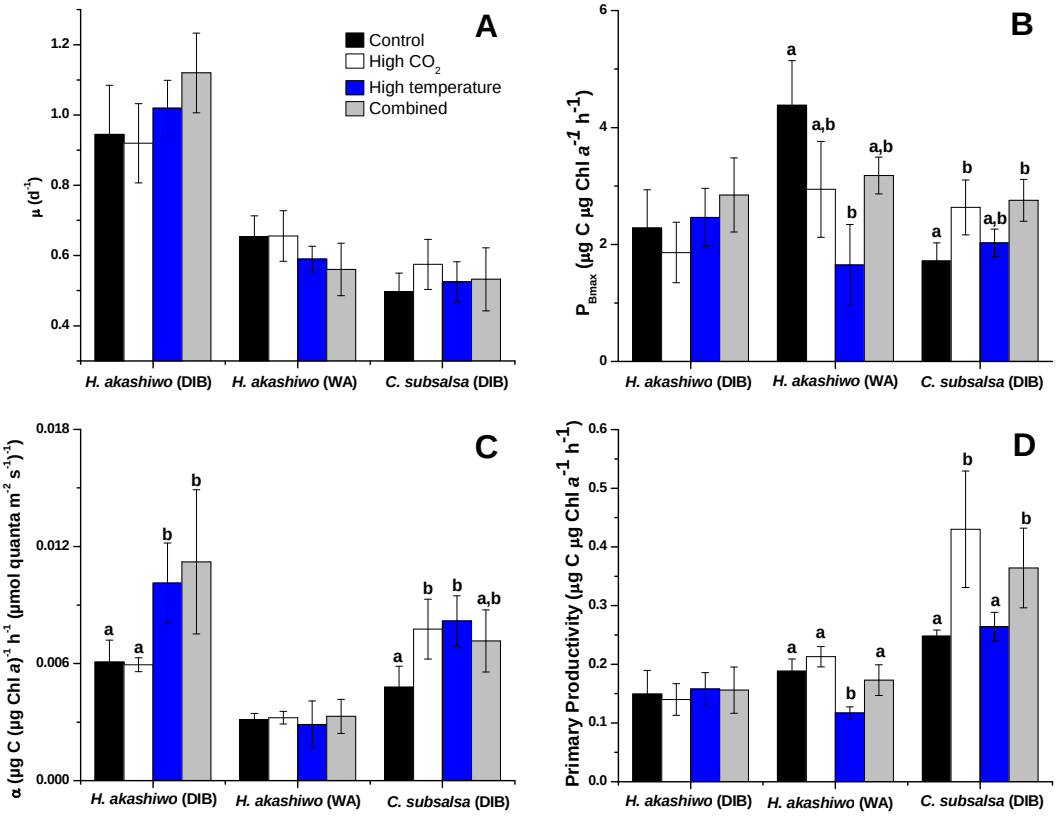

Figure 2.1 **Cell specific growth rates (A), maximal photosynthesis (B), photosynthetic efficiency (C), and primary productivity (D) of *H. akashiwo* (DIB), *H. akashiwo* (WA), and *C. subsalsa* (DIB) in the four temperature and CO_2 treatments. Error bars denote standard deviation (n = 3) and different letters represent significant difference within each strain ($p < 0.05$).**

2.3.2 Chlorophyll fluorescence

There was a small yet significant decline in maximal quantum efficiency (F_v/F_m) in the DIB *H. akashiwo* from 25 °C to 30 °C which recovered with the addition of CO_2 (Fig. 2.2A). The functional absorption cross section (σ_{PSII}) decreased from control levels at elevated temperatures and was significantly lower in the combined treatment (Fig 2.2B). Despite this, there were no significant changes in chl *a* cell^{-1} between any of the four treatments (Table A.1). DIB *H. akashiwo* connectivity (ρ) significant decreased at 30 °C, but the combination of elevated temperature and CO_2 induced a slight recovery (Fig. 2.2C). In contrast there was no effect of elevated temperature, CO_2, or the combination of the two on tau (τ) (Fig. 2.2D). A decline in non-photochemical quenching (NPQ) across all treatments was seen for the DIB *H. akashiwo* but only became significant in the combined treatment in comparison to control levels (Fig. 2.3A). In contrast, the maximal quantum yield (Φ_{max}) did not differ from control levels in any treatment, although 25 °C plus elevated CO_2 values were significantly lower than those at 30 °C plus elevated CO_2 (Fig. 2.3B). A significantly positive correlation was observed between P_{Bmax} and σ_{PSII}' ($r = 0.62$, $p < 0.02$, Fig 2.4A)

The Puget Sound strain of *H. akashiwo* had a similar trend in F_v/F_m as the DIB strain with a slight, but significant, decrease at elevated temperatures (Fig. 2.2A). The σ_{PSII} significantly increased with elevated CO_2 at 25 °C but showed no differences across all other treatments in comparison to control values (Fig. 2.2B). Chl *a* cell^{-1} significantly increased in cultures grown at 30 °C, with or without CO_2 addition (Table A.1). There was a significant increase in ρ across all treatments compared to the control, but no change in τ (Fig. 2.2C, D). NPQ of the Puget Sound *H. akashiwo* significantly decreased at elevated temperatures and elevated CO_2, and no change was

seen in Φ_{max} across all treatments (Fig. 2.3A, B). Unlike the DIB isolate, the Puget Sound *H. akashiwo* exhibited a significantly negative correlation of P_{Bmax} and σ_{PSII}' ($r = -0.583$, $p < 0.05$, Fig.2.4 B)

In contrast to the two *Heterosigma* strains, F_v/F_m of *C. subsalsa* showed a significant decline only with elevated CO_2 under both temperature treatments (Fig. 2.2A). However, σ_{PSII} was more sensitive to temperature with a significant decline under elevated temperature and the combined treatment, although no changes were measured in chl *a* cell^{-1} (Fig. 2.2B, Table A.1). There was no significant difference in ρ, compared to control levels, under all treatments. However, ρ values at 25 °C plus elevated CO_2 were significantly higher than those at elevated temperature with or without CO_2 addition (Fig. 2.2C). Decreases in τ with the addition of CO_2 at both temperatures were noted, although no treatments were significantly different than control rates (Fig. 2.2D). NPQ significantly increased under elevated temperatures and Φ_{max} increased across all treatments, although differences were only significant at 30 °C plus ambient air (Fig. 2.3A and B). Comparing P_{Bmax} vs σ_{PSII}' revealed a distinct difference between temperature treatments. When considered as two different populations, σ_{PSII}' under both temperatures showed a positive correlation with P_{Bmax} but was only significant at 30 °C ($r = 0.863$, $p < 0.02$, Fig. 2.4 C).

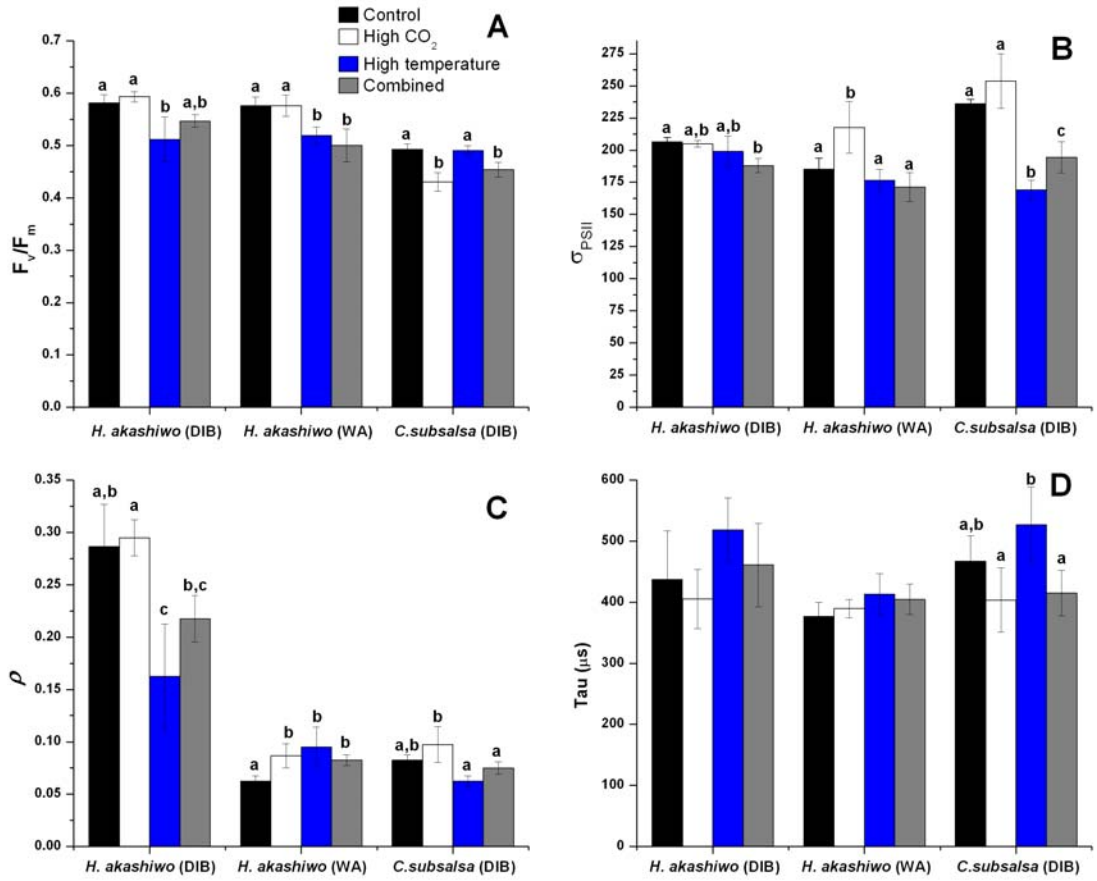

Figure 2.2 **Maximal quantum efficiency of PSII (A), functional absorption cross section (B), connectivity (C), rate of PSII reoxidation (D) in *H. akashiwo* (DIB), *H. akashiwo* (WA), and *C. subsalsa* (DIB). Error bars denote standard deviation (n = 3) and different letters represent significant difference within algal strain (One-way ANOVA, $p < 0.05$). Note: F_v/F_m and σ_{PSII} were analyzed with FIRePro and ρ and Tau were analyzed with FIReWorx.**

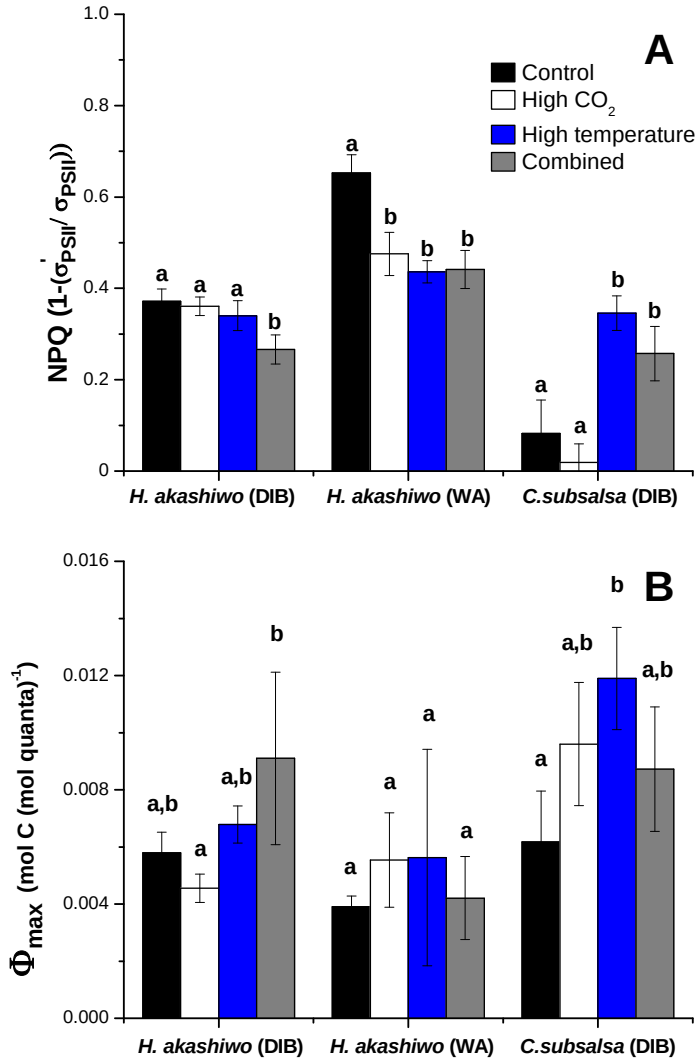

Figure 2.3 **Non-photochemical quenching (A) and maximal quantum yield (B) in *H. akashiwo* (DIB), *H. akashiwo* (WA), and *C. subsalsa* (DIB). Error bars denote standard deviation (n = 3) and different letters represent significant difference within algal strain (One-way ANOVA, $p < 0.05$).**

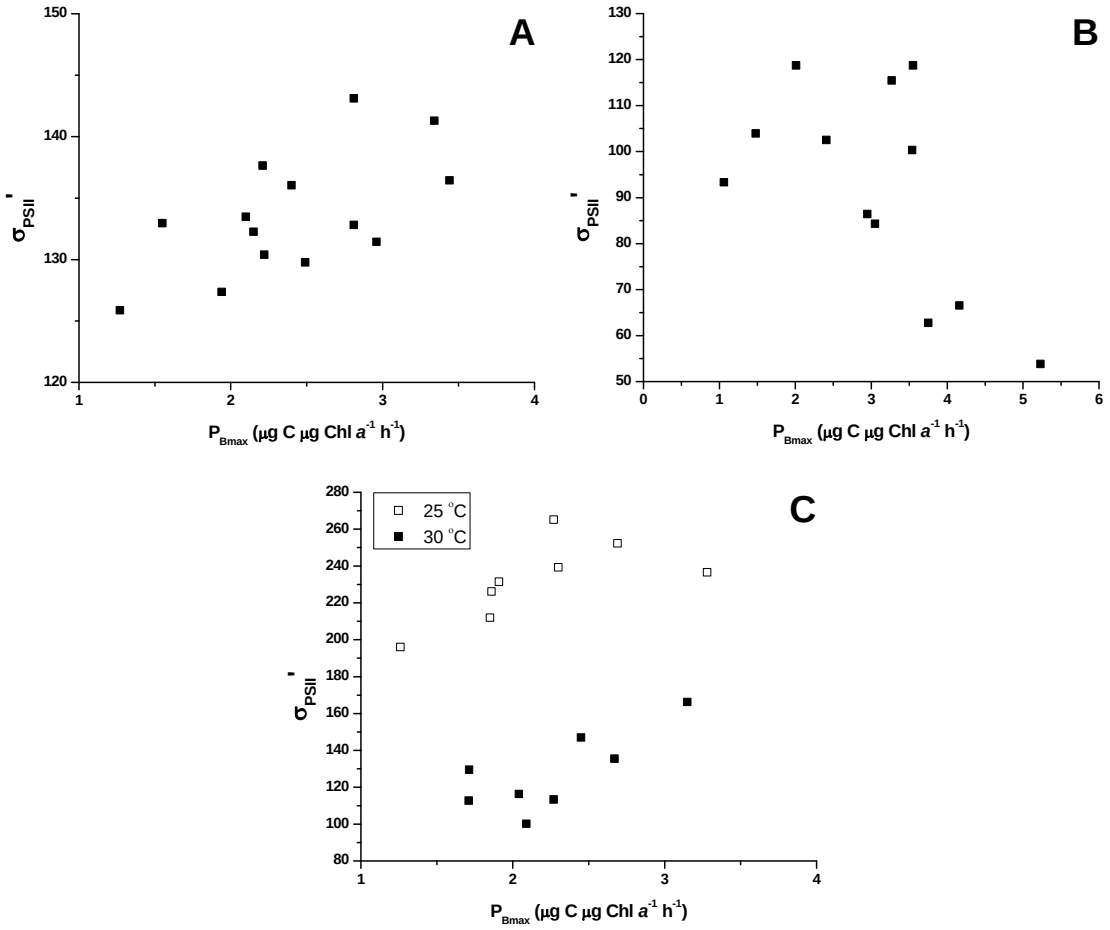

Figure 2.4 **Scatter plots of σ_{PSII}' vs P_{Bmax} in *H. akashiwo* (DIB) (A), *H. akashiwo* (WA) (B), and *C. subsalsa* (DIB) (C). Data points include all temperature/CO_2 treatments: 25 °C + 375 ppm CO_2, 25 °C + 750 ppm CO_2, 30 °C + 375 ppm CO_2, and 30 °C + 750 ppm CO_2. Note: different scales used between panes for clarity in data presentation.**

2.4 DISCUSSION

Although this experiment was originally approached from the focus of understanding how ocean acidification scenarios may impact algal physiology, it became evident that there are many pitfalls associated with altering seawater carbon chemistry, and in particular, in maintaining a constant pCO_2 while still investigating environmentally relevant cellular concentrations found in a typical harmful algal bloom (Rost et al. 2008; Hurd et al. 2009). For example, in these long-term experiments cell number of each culture was held at a relatively high concentration (Table A.1). High algal biomass in a closed system can result in significant shifts in the seawater DIC chemistry especially when the rate of carbon draw down exceeds the supply rate. This can cause a decrease in pCO_2 with a corresponding rise in pH resulting in changes to the initial experimental constraints on carbon chemistry as seen here (Table A.1). Media preparation contributed further to reducing the total pCO_2, as dilutions with purified freshwater for salinity correction and sterilization by autoclaving resulted in decreasing the DIC by 500µM and 300µM respectively (data not shown).

Additional short-term experiments, lasting ten days, under the same CO_2 conditions of 375 ppm and 750 ppm were conducted with DIB *H. akashiwo* at 25 °C and showed a significant dependence of P_{Bmax} on culture biomass in which lower cell numbers resulted in higher levels of chl *a* based carbon assimilation (Fig. A.3). This dependence provides firm evidence for carbon limitation when cultures are at bloom levels, even under semi-continuous methods. However there was still no effect of CO_2 addition on *H. akashiwo* (DIB), similar to the long-term results, regardless of cell

densities and a significant draw down of pCO_2 was again observed across all culture treatments (Table A.4). pH controlled chemostats could be used to overcome the limitations imposed by semi-continuous methods on definitively defining phytoplankton as growing in steady state under continuous pCO_2 levels. As a result of the observed CO_2 draw down in our cultures due to high cell density, this experiment should be considered as a carbon addition experiment, similar to the PeECE III mesocosm experiment, in which we maintained bloom level cell numbers and allowed for the draw down of CO_2 to occur accordingly as in a natural system (Engel et al. 2008; Schulz et al. 2008; Egge et al. 2009).

The objectives of this study were to determine the physiological responses of three different harmful bloom raphidophyte species in response to long-term increases in temperature, CO_2 addition, and temperature and CO_2 addition in concert. A number of parameters, including carbon assimilation, photosynthesis, growth, and PSII photochemistry, were used to evaluate the responses of *H. akashiwo* (DIB), *H. akashiwo* (WA), and *C. subsalsa* (DIB) under bloom conditions of high cell density. Previous work comparing niches of the sympatric DIB species *H. akashiwo* and *C. subsalsa* revealed *Heterosigma* to be the more plastic of the two microalgae in terms of its range and tolerance to salinity and temperature, although both algae could maintain maximal growth at 30 °C (Zhang et al. 2006). In contrast, the Puget Sound is reported to have average winter temperatures of 7.2 °C to 12.8 °C in the summer and the growth range for the *Heterosigma* isolate from this area was previously noted to be from 11 – 16 °C (Staubitz et al. 1997). Considering these known temperature tolerances of each strain, one may hypothesize that the DIB *Heterosigma*, under the experimental conditions tested here, would have a higher growth rate than the Puget

Sound isolate, and this appears to be the case. However, there was only a slight decline in growth rate in the WA isolate at 30 °C relative to 25 °C, thus providing some evidence that this particular alga shows minimal genotypic constraints for growth at temperatures much higher than the waters it was originally collected from. It is also interesting to note that the growth rates reported here for the DIB *H. akashiwo* isolate at 30 °C are faster than those reported in earlier work with or without CO_2 supplementation at 25 °C (Zhang et al. 2006; Fu et al. 2008).

Previous studies of these particular species have only considered the effects of elevated temperature or carbon individually, with only one study examining the effects of short-term exposure to combined increases in temperature and carbon on the DIB strain of *H. akashiwo* (Clark and Flynn 2000; Zhang et al. 2006; Fu et al. 2008). Fu et al. (2008) noted a significant increase in growth rate and maximal photosynthesis in this alga when under the combined conditions of 24 °C and 750 ppm CO_2 in comparison to the control treatments of 20 °C plus 375 ppm CO_2. The lack of evidence for a CCM in this species has led to the suggestion that increased CO_2 may allow for increased carbon fixation and growth, potentially allowing it to outcompete co-existing algae (Nimer et al. 1997). We utilized the same CO_2 treatments as Fu et al. (2008) but with a shift in temperature range to 25 and 30 °C and found no change in the growth and chl *a* based carbon assimilation (Fig. 2.1 A and B). It should be noted, however, that the experimental design used to assess growth rate between Fu et al. (2008) and this current work are different, with the former utilizing a growth rate adjusted semi-continuous strategy and the latter more closely approximating the theoretical maximum growth (μ_{max}) from the early phase of the batch growth cycle. Likewise, while this work is not easily comparable to the study by Fu et al. (2008) due

to the differences in experiment duration, nutrient regimes, and temperature ranges used, it can be assumed that the results under control and elevated CO_2 conditions (25 °C + 375 ppm CO_2 and 25 °C + 750 ppm CO_2) used here should be similar to those of the elevated temperature and combined conditions (24 °C + 375 ppm CO_2 and 24 °C + 750 ppm CO_2) used in their experiment. However, this is not the case for many of the parameters. For example, although the P_{Bmax} is not significantly different across studies, the α under long-term conditions is an order of magnitude lower than under short term conditions (compare Fu et al. (2008) Table 1 vs. Fig 2.1B and C) indicating the maintenance of carbon assimilation despite the decrease in photosynthetic efficiency. In essence, the acclimation time to abiotic parameters can also be thought of as an additional experimental factor in this unique study.

With the exception of the photosynthetic efficiency, PSII connectivity, and non-photochemical quenching, there were marginal changes in many of the measured parameters in the DIB *H. akashiwo* under any temperature/CO_2 combination, in comparison to the control treatment. The effects of temperature were more evident than those of CO_2 with α increasing and NPQ decreasing in response to temperature alone (Fig. 2.1C, Fig. 2.3A). While the rise in carbon fixation with elevated temperature or elevated temperature and CO_2 was not significant, this result is suggestive of a relaxation of energy dissipation via NPQ as carbon fixation rises (Fig. 2.1B). Likewise, while total chl *a* content did not change significantly with temperature, there was an evident increase in the chlorophyll specific absorption coefficient (a*, Table A.1 and Fig. A.1). This corresponds to the elevated efficiency of carbon fixation seen in the rise of α in the photosynthetic to irradiance response, which is dependent on light absorption, and the positive correlation of light harvesting

ability and carbon fixation (Fig. 2.1C and Fig. 2.4A). The decrease in connectivity (ρ) at higher temperatures represents a decrease in the energy transfer between PSII reaction center complexes, possibly in response to a more fluid thylakoid membrane or a change in other photosynthetic pigments not measured here such as the carotenoid fucoxanthin (Falkowski and Raven 2007).

A study by Gordillo et al. (2003), working with the chlorophyte *Dunaliella viridis*, showed the dependence of carbon assimilation on nutrient levels, with growth and photosynthesis increasing in the presence of higher pCO_2 only under N-replete conditions. Although cells were maintained in semi-continuous conditions during our experiment, final day sampling occurred 48 hours after the last media transfer, thus allowing for the possible draw down of the available nutrients. If cells were becoming nutrient limited at that time, this could explain the lack of significant change in carbon assimilation in the DIB *H. akashiwo* (Fig. 2.1 B). The significant effect of cell density on chl *a* based carbon assimilation noted from the short-term pilot study with low cell concentrations provides evidence for possible carbon and nitrogen limitation in the long-term cultures (Fig. A.3).

The Puget Sound strain of *Heterosigma* also showed a highly variable photosynthetic response to increased temperature. Although there was no significant change in growth rate when grown in batch culture, both short and long-term carbon assimilation significantly declined at 30 °C but recovered with the addition of CO_2 (Fig. 2.1B and D). Despite the decrease in carbon assimilation at higher temperature, *H. akashiwo* (WA) was able to maintain photosynthetic efficiency and Φ_{max} across all treatments (Fig. 2.1C, Fig. 2.3B). Likewise, although we see a significant drop in F_v/F_m, corresponding with the decline in P_{Bmax} at elevated temperatures, the decrease

in quantum efficiency is not enough to suggest photoinactiviation (Fig 2.2A). Enhanced loss of electron flow, reflected in a decrease in the rate of reoxidation of Q_A attributed to blocked electron flow out of PSII, has been known to occur during light or temperature stress (Pospisil and Tyystjarvi 1999). The lack of change in the reoxidation rate of the PQ pool seen here, as well as the decline in NPQ, both support the suggestion that photoinactivation was not occurring under elevated temperatures (Fig. 2.3A, Fig. 2.2D).

The observed up-regulation in connectivity between photosystems, the decrease in NPQ, and the significant increase in σ_{PSII}' could have aided in maintaining adequate light harvesting for photochemistry and photosynthetic efficiency under the stress of higher temperatures (Fig. 2.2 C, Fig. 2.3 A, Table A.2 and Fig A.2 B). This is also evident in the negative correlation of σ_{PSII}' and P_{Bmax}, showing the up-regulation of light harvesting when cells are stressed. The significant increase in chl *a* cell^{-1} at elevated temperatures corresponds with this, however the decrease in a* indicates a reduction in the light harvesting effectiveness (Table A.1 and Fig A.1). Thus, elevated chl *a* cell^{-1} resulted in some "package effect" either due to an increase in the number or size of PSU's or an increase in the number of thylakoid membranes causing self-shading to occur (Berner et al. 1989; Falkowski and Raven 2007). However, the increase in photosynthetic pigments at elevated temperatures is hard to reconcile with previous work noting a negative feedback signal to the nucleus to down-regulate synthesis of the LHCII pigment protein complexes when under light or temperature stress (Maxwell et al. 1995). There was no increase in excitation pressure on PSII, as indicated by the effective quantum yield in the light acclimated state, and this could explain why no decrease in chl *a* was seen here, although the rise in chl *a* with

temperature is still a puzzling and open question. While both isolates of *H. akashiwo* increased their light harvesting ability in response to temperature, positive effects of up-regulating σ_{PSII}' reflected by changes in P_{Bmax} (Fig. 2.4A and B) were noted only in the DIB isolate.

In contrast to both isolates of *Heterosigma*, *C. subsalsa* exhibited responses to both temperature and CO_2 addition. Although there was no significant change in growth between any treatments, carbon assimilation, primary productivity, and electron transport rate significantly increased with the addition of CO_2 under both temperatures (Fig. 2.1A and B, Fig. 2.2 D). Elevated CO_2 alone had a slight, yet insignificant, positive effect on the light harvesting capabilities (Fig 2.2 B) of *C. subsalsa*, suggesting that the increase in P_{Bmax}, and the corresponding increase in α and Φ_{max}, could have been primarily a result of the small rise in connectivity and the increase in the rate of reoxidation of the PQ pool. In contrast, elevated temperature appeared to increase the excitation pressure placed on PSII as seen by the significant decline in effective quantum yield in the light adapted state (Fig A.2 A). This may have resulted in the significant increase in NPQ and the decrease in light harvesting capability seen at elevated temperatures (Fig. 2.2B, Fig 2.3A). However, elevated CO_2 still resulted in an increase in the target area for light capture and an equivalent rise in carbon fixation, regardless of temperature (Fig 2.1B, Fig 2.2 B).

The effect of temperature on algal growth and metabolism is perhaps one of the most widely studied environmental factors due to its ease of measurement. In general, algae acclimatized to temperatures below their optimum will exhibit an increase in growth when switched to higher temperatures (Raven and Geider 1988). Temperature controlled constraints of photosynthesis will decline, and can manifest as

an increase in Rubisco activity, carbon fixation, and light harvesting (Coles and Jones 2000; Staehr and Birkeland 2006; Fu et al. 2008). However, when cells acclimated to optimal temperatures are switched to higher temperatures no change in growth, or even a decline in growth rate will occur (Atkin and Tjoelker 2003; Staehr and Sand-Jensen 2006). Higher metabolic rates lead to a greater demand for reductant energy from the light reactions and nutrients, increasing the chance for carbon fixation inhibition and nutrient limitation. The long-term acclimation to temperature used here could explain why there was no significant response in growth rates observed at higher temperatures. However, we can begin to see a decline in the Puget Sound *H. akashiwo* growth, indicating possible photoinhibition at temperatures past 30 °C in this cold water isolate as well as significant energy loss due to elevated respiratory demand (Fig. 2.1A).

The effects of elevated pCO_2 on algal growth and physiology have proven to not be as straightforward as temperature. It is suggested that phytoplankton are not limited by current levels of pCO_2 due to the development of efficient CCMs in many speciess (Tortell et al. 2000; Falkowski and Raven 2007). Therefore any increases in atmospheric carbon dioxide should have little to no effect on carbon fixation and subsequent growth. However, a number of short-term studies have shown an array of cellular changes at elevated CO_2 in several phytoplankton taxa including, but not limited to, the cyanobacteria *Trichodesmium* (Hutchins et al. 2007; Levitan et al. 2007), *Synechococcus* spp., *Prochlorococcus* spp. (Fu et al. 2007), and *Nodularia spumigena* (Czerny et al. 2009) the chlorophyte *D. viridis* (Gordillo et al. 2003), the raphidophyte *H. akashiwo*, the dinoflagellate *Prorocentrum minimum* (Fu et al. 2008), and the coccolithophore *E. huxleyi* (Delille et al. 2005). In contrast, a long-term study

by Collins and Bell (2006) comparing *Chlamydomonas*, isolated from the soil of natural CO_2 springs and strains from laboratory populations grown over 1000 generations at elevated CO_2, has shown the insensitivity of growth rates to CO_2 in both strains.

From these various uni-algal experiments we can begin to predict physiological changes that will occur under elevated temperature and CO_2 conditions. However, it is only when working with natural plankton communities that we can begin to understand how a global climate change scenario will effect blooms and species competition. A short vs. long-term study on a natural community inoculated with the calcifying coccolithophore *Pleurochrysis carterae* showed a decrease in the impact of elevated pCO_2 over time on calcification with no effect on the ecology of non-calcifying groups (Casareto et al. 2009). Since all groups responded positively to the elevated pCO_2 there was no net change in the phytoplankton community. This was also found in the PeECE III experiment where although the dominant species in the community changed over time throughout the rise and decline of the bloom, neither phytoplankton composition nor succession differed between CO_2 treatments (Egge et al. 2009). In contrast, a study by Feng et al. (2009) showed large differences in community structure across treatments as well as net increases in P_{Bmax} at elevated temperature and elevated temperature and CO_2. Microzooplankton abundance and physiology were also monitored during this shipboard experiment (Rose et al. 2009). They suggested that a shift in community structure to an unpalatable phytoplankton assemblage dominated by coccolithophores in the elevated temperature/CO_2 treatments had a larger impact on the decline in microzooplankton abundance than physiological changes due to temperature or CO_2.

The effects of bloom assemblage on co-existing microalgae and plankton are not limited to just heterotrophic interactions but are also impacted by changes in available nutrients, light, and oxygen. When blooms collapse, large areas of anoxia can occur due to bloom decomposition by bacteria, light can be severely attenuated when blooms form on the surface, and nutrients can either be depleted during the rise of a bloom or returned to the water column when they collapse. There is also evidence that the release of dissolved organic carbon (DOC) could act as a sink mechanism in order to protect the photosynthetic mechanisms when products can not be metabolized or stored (Gordillo et al. 2003; Engel et al. 2004). Thus, the increase in DOC to the system can also act as a nutrient source for the co-existing microbial and plankton community (Sunda et al. 2006; Michaloudi et al. 2009). The lack of change in growth rates and cell size (data not shown) across all temperature/CO_2 conditions for any of the three raphidophytes studied here suggests that cells could potentially be storing carbon, or as found by Engel et al. (2004) in *E. huxleyi*, releasing it as DOC. Thus, although elevated temperature and CO_2, within the ranges studied here, will most likely not change raphidophyte bloom dynamics, their effects on cell physiology and the potential DOC release, could play an important role in the succession of co-existing species.

Chapter 3

THE POTENTIAL USE OF THE NITRATE REDUCTION PATHWAY AS A DISSAPATING MECHANISM FOR EXCESS EXCITATION ENERGY IN THE RAPHIDOPHYTE *HETEROSIGMA AKASHIWO*

ABSTRACT

During transient periods of elevated irradiance and temperature phytoplankton are inherently subjected to damage to their photosynthetic mechanisms due to imbalances between the light reactions and carbon fixation. Hence, they have evolved a number of mechanisms to dissipate excess excitation energy through alternative pathways such as the Mehler reactions, photorespiration, and enhanced mitochondrial respiration. Likewise, previous work with diatoms has found evidence for the use of the Nitrate Reductase (NR) Pathway as a potential sink for excess electrons, through its use of NAD(P)H, during cold water and high light periods. Preliminary evidence for the use of the NR pathway to dissipate excess excitation energy in the raphidophyte *Heterosigma akashiwo* is presented in this study. Through the use of single and multiple turnover fluorometers, the photosynthetic electron transport rate (ETR) was measured in cells grown with nitrate or ammonium as their primary N-source. Cultures were also subjected to shifts from low (60 µmol quanta $m^{-2}s^{-1}$) to high light (785 µmol quanta $m^{-2}s^{-1}$) and ETR monitored over a 7-day period. Initial results from cultures grown under low light showed significantly higher ETR in cells grown on nitrate vs. those grown with ammonium. However, subsequent experiments with shifts to high light were not in agreement and large error between

replicates made analysis difficult. Likewise, any significant increases in ETR found could not be solely attributed to a sink provided by the NR pathway by the techniques utilized here.

3.1 INTRODUCTION

A fundamental theme in phytoplankton research is the study of abiotic and biotic impacts on algal physiology. In particular, the ability of cells to acclimate to transient levels of light, temperature, and nutrients represents one of the key factors in maintaining balance between light absorption and carbon assimilation. Differences in this ability between species play a large role in the competitive dominance in a mixed algal community. This becomes especially important in light of reports of increasing frequency and duration of harmful algal blooms (HABs) and their correlation to elevated temperature, light and anthropogenic eutrophication (Anderson et al. 2002; Hallegraeff 2003; HARRNESS 2005).

Photoautotrophs have developed a number of mechanisms to acclimate to imbalances between light absorption and carbon assimilation. The primary strategy involves the light harvesting complexes (LHC), with cells either decreasing concentrations of light harvesting pigments, increasing photoprotective pigments such as xanthophylls and carotenoids, or shading photosynthetic components by accumulating UV-absorbing pigments (Marshall and Newman 2002; Harris et al. 2005; Falkowski and Raven 2007). However, when exposed to long periods of excessive irradiance these physiological changes are not always sufficient and alternative pathways of light energy dissipation are utilized. These include the Mehler reaction, photorespiration, or utilization of the reductant NAD(P)H, produced from the photosynthetic electron transport chain (ETC), by the enzyme nitrate reductase (NR).

Light energy absorbed by pigments in the LHC is transferred linearly through the photosynthetic ETC beginning with the oxygen evolving complex, which oxidizes H_2O and releases O_2 and protons, coupled to photosystem II (PSII). Electrons then pass through a series of redox carriers starting with the plastoquinone (PQ) pool, the cytochrome (cyt) b_6f complex, and plastocyanin, before finally being transferred to photosystem I (PSI). These carriers also act to shuttle protons across the thylakoid membrane establishing an electrochemical gradient utilized by the chloroplast ATP synthase. Electrons arriving in PSI are transferred to either ferridoxin (Fd,) which in turn reduces $NADP^+$ to NADPH needed for the fixation of CO_2, or are shuttled into a cyclic flow around PSI. Cyclic flow utilizes the same carriers as linear transfer starting by transferring electrons back to the PQ pool. Thus this pathway produces no net reduction of Fd or $NADP^+$ while continuing to shuttle protons across the thylakoid membrane for the synthesis of ATP (Falkowski and Raven 2007).

The Mehler reactions, also known as the water-water cycle, takes advantage of the cyclic electron flow around PSI by using the electrons from the oxidation of H_2O at PSII to reduce O_2. Photoreduction of O_2 produces super oxide radicals ($O_2^{-\bullet}$) and H_2O_2 which are quickly rendered harmless via superoxide dismutase and the ascorbate peroxidase pathway, respectively, to produce H_2O (Asada 1999; Asada 2000; Makino et al. 2002). Thus, this pathway is suggested as a photoprotective mechanism due to its ability to scavenge reactive oxygen species and its tight control over the ATP-NADPH ratio (Asada 2000).

Another energy dissipation mechanism utilized by photoautotrophs is photorespiration, or the light-dependent consumption of O_2 by ribulose bisphosphate carboxylase oxygenase (RuBisCO). Both carbon dioxide and oxygen are viable

substrates for the enzyme RuBisCO, however when oxygen is used as a substrate carbon is fixed at a reduced rate with a higher metabolic cost. Although normally considered the more inefficient pathway, photorespiration represents another potential electron sink during periods of harmful excess excitation energy due to irradiance or temperature stress (Portis and Parry 2007).

Lastly, the use of the reductant NAD(P)H by NR to assimilate nitrate has also been suggested as an alternative electron sink (Lomas and Glibert 1999; Parker and Armbrust 2005). Reliant upon the presence and abundance of nitrogen in the environment, this pathway reduces nitrate to nitrite, via the enzyme NR and energy from the reductant NAD(P)H. Lomas and Gilbert (1999), using cold water diatom dominated blooms from the Chesapeake and Delaware Bays, observed uptake rates of NO_3^- in excess of nutritional requirements. This, along with the observation of increased transcript abundance of NR under high light in the diatom *Thalassiosira pseudonana* by Parker and Armbrust (2005), provides evidence for the use of this pathway under the stress of low temperature or high light. Although the use of this pathway as an electron sink has only been documented in diatoms, observations of high NR activity in the HAB species *Heterosigma akashiwo* (J. Stewart & K. Coyne, personal observations) warrants further study of this potential electron bleed. By growing cells with either ammonium, effectively eliminating the necessary substrate for the NR pathway, or nitrate as a nitrogen source and observing the changes in electron transport rates (ETR) through the PSII we can begin to validate the potential use of this pathway to dissipate excess excitation energy.

3.2 METHODS

3.2.1 Isolates and culture conditions

Heterosigma akashiwo (CCMP 2393) was originally isolated from Torquay Canal, Rehoboth Bay, Delaware, and deposited at the Center for the Culture of Marine Phytoplankton (https://ccmp.bigelow.org/home) (CCMP). Cultures were maintained at 25 °C under a 12:12 h light dark cycle with an irradiance of 60 µmol quanta $m^{-2}s^{-1}$ provided by cool white fluorescent lamps. Replicates (n=4) were grown in modified f/2 medium using offshore seawater diluted to a salinity of 26 ‰. Treatments were defined by differing nitrogen sources of either $NaNO_3$ at a final concentration of 200 µM or NH_4Cl at a final concentration of 150 µM.

3.2.2 Experimental design

Three separate experiments using replicate (n = 4) cultures were grown in 500 ml Erlenmeyer flasks sealed with a silicone stopper retrofitted with borosilicate inlet and outlet glass rods. Ambient air was pumped through the inlet rod to gently bubble cultures and the outlet rod was stuffed with cotton allowing for a sterile environment. The first experiment was conducted after 7 days of semi-continuous growth (50% media transfer every 2 days) under four separate growth conditions as follows: nitrate as the nitrogen source, nitrate as the nitrogen source plus aeration with ambient air, ammonium as the nitrogen source, and lastly ammonium as the nitrogen source plus aeration with ambient air. On day 7 samples were collected from each replicate and multiple turnover fluorescence was measured by Pulse Amplitude Modulation (PAM) fluorometery as described below (PAM 101, Walz, Germany).

The second experiment held cultures in semi-continuous growth for two weeks, with aeration of all cultures beginning on day 7. At the end of the two weeks

cultures were shifted from an irradiance of 60 µmol quanta m^{-2} s^{-1} to 785 µmol quanta m^{-2} s^{-1}. The photosynthetic response was followed by PAM fluorometry, as in experiment one, at 2, 4, 6, and 10 hours after the shift to high light and subsequently 1, 2, 3 and 7 days at high light. To further investigate the role of NR and electron transport, sodium tungstate (Na_2WO_4), an inhibitor of NR, was added to NO_3^- sub-cultures (0.02 M) on day 7 (Miyagi et al. 1992). After a four hour incubation, starting with the beginning of the light cycle, cultures were again sampled with PAM fluorometry.

In the third and final experiment cultures of *H. akashiwo* were grown semi-continuously with aeration for 7 days prior to any light shifts. Simultaneous fluorescence measurements were taken 2, 6, 8, 10, and 24 hours after a shift to 785 µmol quanta m^{-2} s^{-1} using the PAM and a Fluorescence Induction and Relaxation (FIRe, Satlantic) instrument. Sodium tungstate was again added to sub-samples of NO_3^- grown cells to a final concentration of 0.02 M and fluorescence measured 4 hours after the shift to high light.

3.2.2 Fluorescence analysis

PSII activity was monitored on the PAM using a 1.5 ml sub-sample of culture between 09:00 and 11:00 h, unless otherwise noted, to account for any diel periodicity in results. Samples were first dark acclimated for two minutes before measuring the maximum quantum yield of PSII fluorescence (F_v/F_m) with a brief saturation pulse provided by blue LED array. The difference between the steady state fluorescence (F_o), and maximal fluorescence (F_m) read during the first pulse of light, was used to calculate the variable fluorescence (F_v). F_v/F_m, or the maximum quantum yield of PSII, is an indication of PSII efficiency (Butler 1978; Baker 2008). After

steady state fluorescence (F_o) was recovered (approximately 5 minutes) the sample was exposed to an actinic light set at 100 µmol quanta $m^{-2}s^{-1}$ for 5 minutes before another saturation pulse of light was used to measure the effective quantum yield of PSII ($\Delta F/F_m'$) in the light adapted state. The sample was then left in the dark for 30 seconds before the start of a rapid light curve (RLC) protocol consisting of 20 second actinic light steps of 50, 90, 165, 274, 408, 568, 719 and 943 µmol photons $m^{-2}s^{-1}$ followed by a 400 ms saturation light pulse at the end of each light step to record $\Delta F/F_m'$. The electron transport rate (ETR) was calculated as:

$$ETR = \frac{\Delta F}{F_m'} \times E \times \frac{A}{2}$$

where E is the incident PAR and 2 represents the minimum absorption of 2 photons for transport of one electron from PSII to PSI. A is the absorptance of the algal suspension calculated from the absorption spectra of the sample measured using a spectrophotometer outfitted with an integrating sphere (Shimadzu 2401) using the following equation:

$$A = 1 - 10^{-OD}$$

where OD is the average optical density between 440 nm and 500 nm. ETR curves were fit using the hyperbolic tangent function from Jassby and Platt (1976) and normalized to cell number. Cells from each sample were quantified using a Neubauer hemocytometer.

During experiment three simultaneous fluorescence measurements were conducted using the FIRe instrument. Single turnover fluorescence of intact cells was measured by applying a 100 µs flash of blue light, followed by a series of flashes over 500 ms to record the reoxidation of the Q_A quinone in PSII. After this relaxation

period multiple turnover fluorescence was measured by applying a long pulse of light for 20 ms in order to saturate the PSII and PQ pool. The protocol ended by applying a weak light for one second to measure the subsequent reoxidation of the PQ pool. After measuring fluorescence under dark adapted conditions, samples were exposed to 5 minutes of light (500 μmol quanta $m^{-2}s^{-1}$) using the separate actinic light source provided by a blue LED array before applying the same measurement protocols as used in the dark. Parameters measured in the light adapted state are indicated by ' (i.e. F_v'/F_m'). PSII photochemistry parameters were determined by fitting the four step fluorescence trace using the FIRePRO software provided by Satlantic Inc. ETR was calculated using the FIRe parameters as follows:

$$ETR_{RCII} = E \times \sigma_{PSII}' \times F_q' / F_v' \times 0.00603$$

where σ_{PSII}' is the PSII effective absorption cross section, F_q'/F_v' is the PSII trapping efficiency, and 0.006023 accounts for conversion of σ_{PSII}' from $Å^2$ $quanta^{-1}$ to m^2 mol $RCII^{-1}$ and E from μmol photon m^{-2} s^{-1} to mol photons $m^{-2}s^{-1}$ (Suggett et al. 2006).

3.2.3 Statistics

All fluorescence parameters and calculated ETR were assessed using a one-way ANOVA, unless otherwise noted, followed by Tukey HSD post hoc testing using SPSS (Version 16.0). Data were assessed for normality and homoscedasticity and when necessary were transformed prior to any statistical analysis. In the event that transformation did not help with distribution or variance, data were evaluated using the non-parametric Kruskal-Wallis test and the Mann-Whitney U post hoc test. Differences were deemed significant when $p < 0.05$.

3.3 RESULTS AND DISCUSSION

For the initial experiment *H. akashiwo* cultures were held at low light and grown under four treatments with either nitrate or ammonium as the N-source and aeration with ambient air or no bubbling. Cultures grown on nitrate with continuous aeration were found to have a significantly higher ETR_{max} than any other treatment ($p < 0.001$, $f = 29.80$, Table 3.1). It is well known that Rubisco has a low affinity for CO_2, thus preferentially binding O_2 and subjecting cells to a metabolically costly carbon fixation pathway. To overcome this many phytoplankton have evolved carbon concentrating mechanisms (CCMs) in order to increase the concentration of CO_2 around Rubisco (Badger et al. 1998). However, since no evidence has been provided for a CCM in *H. akashiwo*, a sensitivity to decreases in CO_2 could potentially explain the lower ETR_{max} seen in non-aerated vs aerated NO_3^- grown cells (Nimer et al. 1997). Despite this, no significant differences in the quantum efficiency were seen, and as F_v/F_m stayed relatively high across all treatments it suggests that cultures were able to maintain photosynthesis regardless of any possible carbon limitation or N-source (Fig. 3.1). However, it is interesting to note the significantly lower effective quantum yield measured in the light acclimated state (F_v'/F_m') of non-aerated nitrate compared to all other treatments (Fig. 3.1, $p < 0.001$, $f = 17.51$). This again is most likely due to the aforementioned carbon limitation thus resulting in an increase in excitation pressure on PSII. Faster uptake of NH_4^+ by *H. akashiwo*, as reported by Herndon and Cochlan (2007), or relief from the increased energy requirement needed to reduce NO_3^-, could explain why the effects of carbon limitation are not seen in cells grown on NH_4^+. The preliminary evidence shown here for significantly higher ETR_{max} in nitrate vs. ammonium grown cells demonstrates how the availability of nitrate in the medium

will directly influences the rate of electron flow through PSII to produce more NAD(P)H in order to reduce nitrate to its usable form of ammonium.

Table 3.1 ETR_{max} of *H. akashiwo* grown with either nitrate or ammonium as a nitrogen source and with or without continuous aeration.

Growth conditions	ETR (μmoles $e^{-}\cdot cell^{-1}\cdot s^{-1}$)
NO_3^-	$5.15\ 10^{-5} \pm 6.50\ 10^{-6}$
NO_3^- + aeration	$8.85\ 10^{-5} \pm 9.57\ 10^{-6}$ *
NH_4^+	$5.43\ 10^{-5} \pm 1.90\ 10^{-6}$
NH_4^+ + aeration	$6.02\ 10^{-5} \pm 2.08\ 10^{-6}$
Superscript (*) denotes a significant difference ($p < 0.01$) in ETR between growth conditions ($n = 4 \pm$ S.D.).	

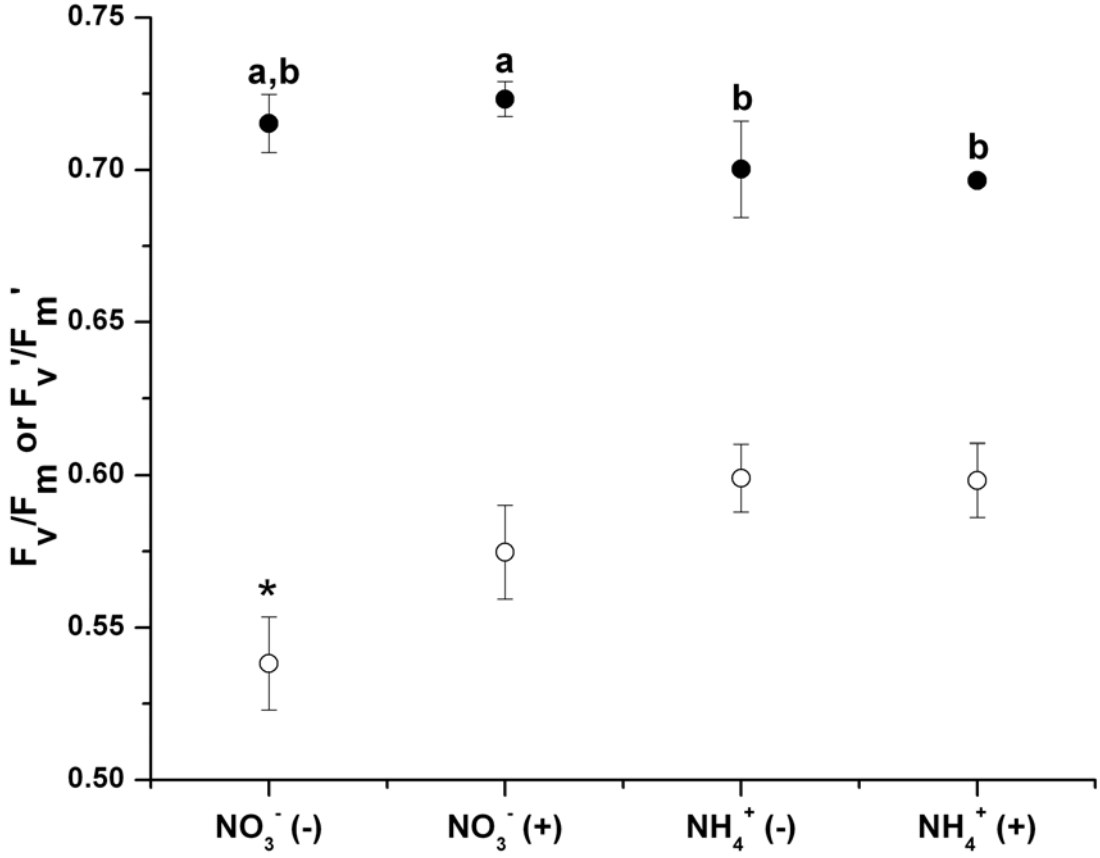

Figure 3.1 **Maximum (closed circles) and effective (open circles) quantum yield of *H. akashiwo* grown on nitrate or ammonium with (+) or without (-) aeration. (*) and letters denote significant difference ($p < 0.05$) using one-way ANOVA (n = 4 ± S.D.) with Tukey's HSD post-hoc test.**

In the second experiment all cultures were aerated to negate any carbon limitation and cultures were subjected to shifts in irradiance from 60 to 785 µmol quanta m^{-2} s^{-1}. There was a significant decline in ETR_{max} during the first six hours of high light exposure under both nitrate and ammonium conditions, but no significant differences between treatments over the initial light shock period until the 10 h mark (Fig. 3.2, $p < 0.001$, $f = 13.48$). Although F_v/F_m significantly declined over the 7-day high light period, this appeared to stabilize by the end of the experiment (Fig. 3.3, $p < 0.001$, $\chi^2 = 27.06$) and as F_v/F_m was still relatively high, this reduction may simply represent more of a photoacclimation response rather than photoinactivation. Thus, the large decrease in ETR_{max} was most likely due to photoacclimative strategies including increases in photoprotective pigments such as xanthophyll and carotenoids or decreases in connectivity between reaction centers in response to over-saturating irradiance (MacIntyre et al. 2000; Baker 2008). Both nitrogen treatments exhibited some recovery after the first dark cycle, but after 48 h, ETR_{max} again declined and subsequently stabilized over the remaining days (Fig 3.2). The addition of sodium tungstate on day 7 to high and low light acclimated nitrate grown cells had no significant impact on ETR_{max}, but resulted in a slight yet insignificant drop in F_v'/F_m' measured under high light (Fig. 3.2, Fig. 3.3). This suggests that the NR pathway may only act as a short term photoprotective mechanism in *H. akashiwo* and may become saturated within 1 to 2 hours or could be indicative of a brief transitory increase in NO_3^- uptake in response to saturating irradiances.

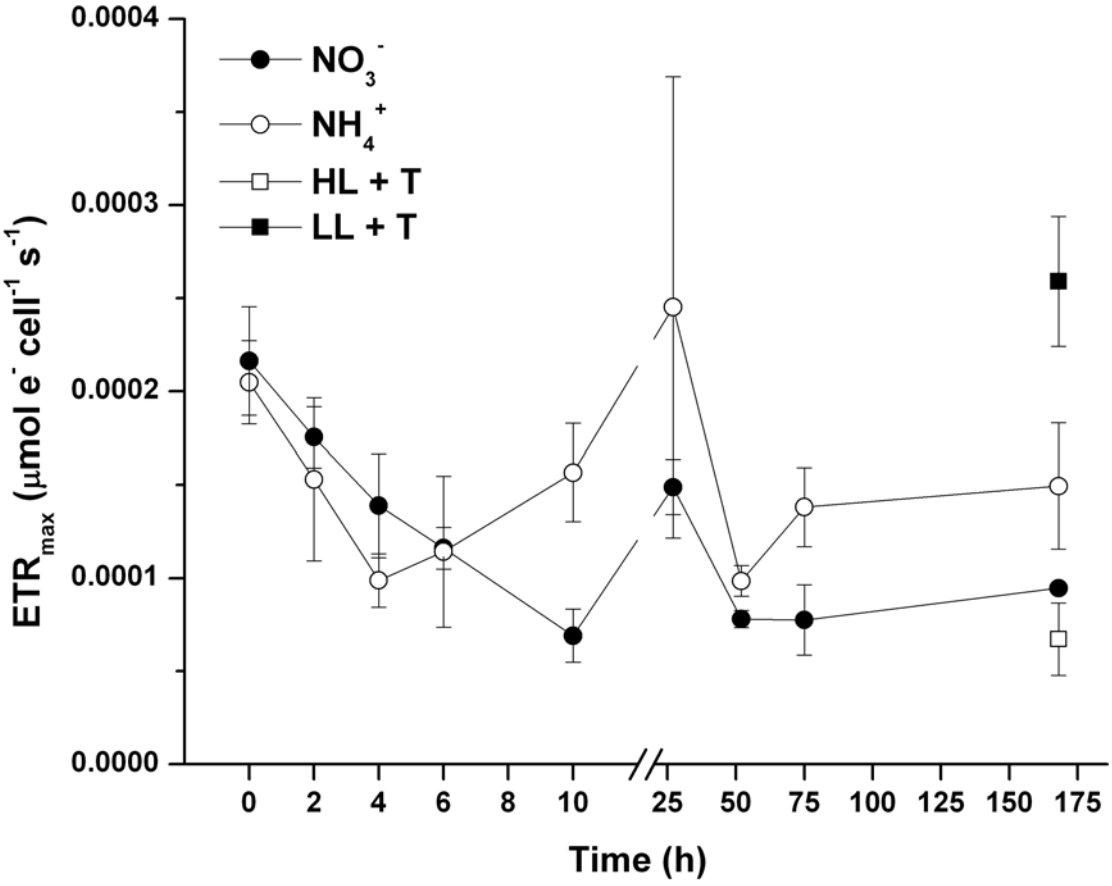

Figure 3.2 **ETR_{max} of *H. akashiwo* grown on NO_3^- and NH_4^+ shifted from 60 to 785 µmoles quanta m^{-2} s^{-1} at time zero. After 7 days (175 h) of semi-continuous growth, sodium tungstate (T) was added to cultures under high light (HL) and low light (LL) conditions. Error bars represent n = 4 ± S.D.**

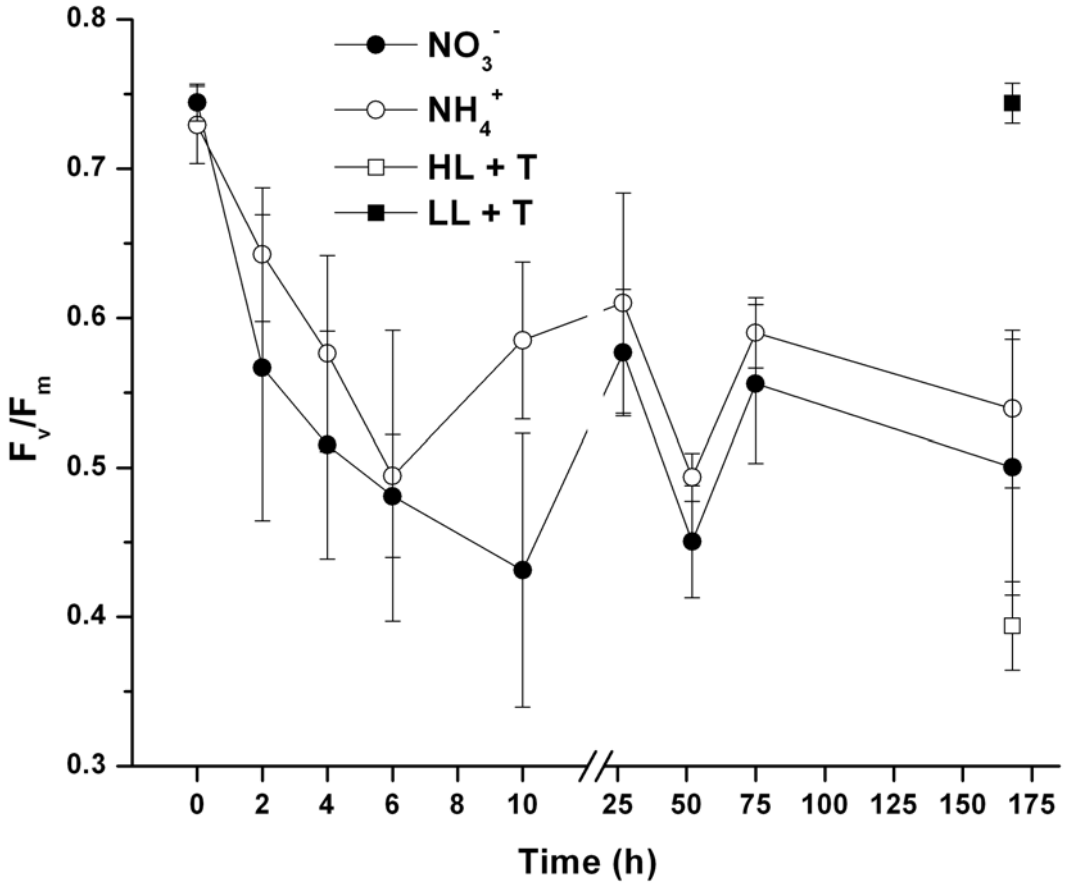

Figure 3.3 **$F_v\backslash F_m$ of *H. akashiwo* grown on NO_3^- and NH_4^+ shifted from 60 to 785 µmoles quanta $m^{-2}s^{-1}$ at time zero. After 7 days (175 h) of semi-continuous growth, sodium tungstate (T) was added to cultures under high light (HL) and low light (LL) conditions. Error bars represent n = 4 ± S.D.**

Simultaneous measurements with two different fluorometers, PAM and FIRe, were conducted in the third and final experiment at 2, 6, 8, 10, and 24 h after shifting NO_3^- and NH_4^+ grown cultures to high light. No significant differences between NO_3^- and NH_4^+ grown cells were noted in the ETR measured either by PAM or FIRe fluorometery (Fig 3.4). Although F_v/F_m , declined over the 24 hour treatment, it stabilized before 10 hours of high light in NO_3^- grown cells, and by 24 hours in NH_4^+ grown cells, again suggesting photoacclimation over photoinactivation (Fig 3.5). However, similar to *Chattonella subsalsa* (Warner and Madden 2007), *H. akashiwo* showed minimal change in non-photochemical fluorescence quenching (NPQ, data not shown), as calculated from FIRe parameters, after the first 2 hours of light shock, suggesting that dissipation of light energy at the light harvesting antennae played a minimal photoprotective role during the prolonged high light exposure whether grown on nitrate or ammonium. Figure 3.6 shows the quick reduction of PSII connectivity during the first two hours of high light suggesting that a decrease in shared electrons between reaction centers could play a large role in the photoacclimation and photoprotection of *H. akashiwo* regardless of nitrogen source.

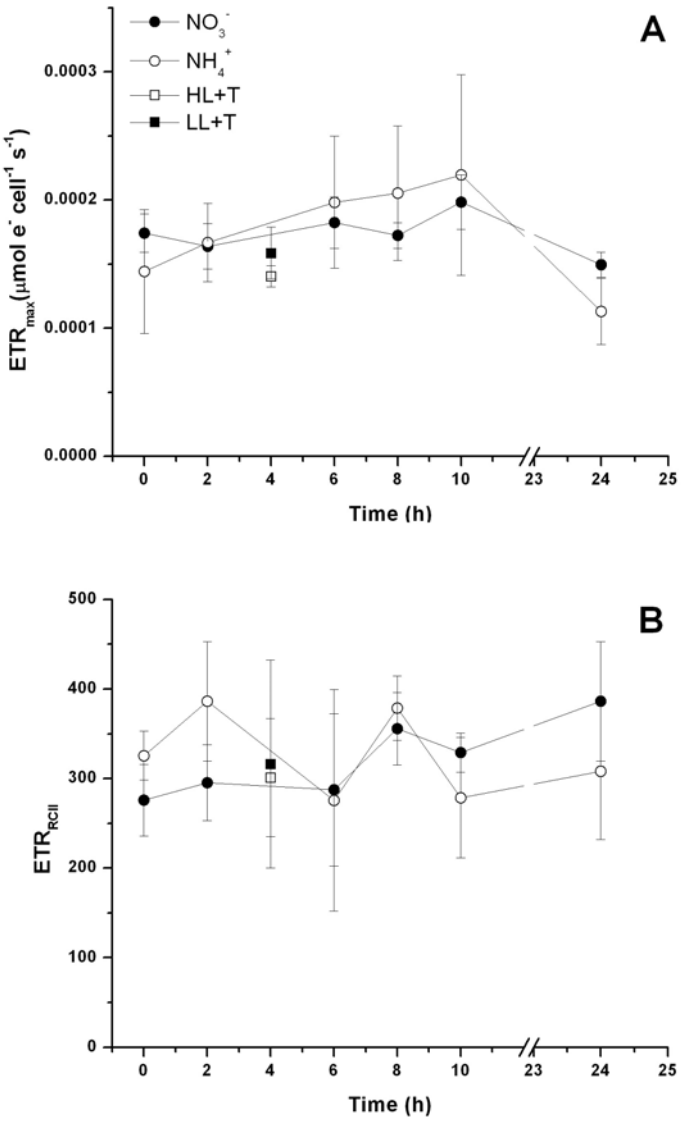

Figure 3.4 **The ETR_{max} and ETR_{RCII} of *H. akashiwo* grown with either NO_3^- or NH_4^+ as the nitrogen source. Cultures were shifted from 60 to 785 µmoles quanta $m^{-2}s^{-1}$ at time zero and fluorescence was measured by (A) PAM fluorescence or (B) FIRe protocols. Sodium tungstate (T) was added to sub-cultures under high light (HL+T) and low light (LL+T) conditions and fluorescence was read four hours after the shift to high light. Error bar denote 1 ± S.D (n = 4).**

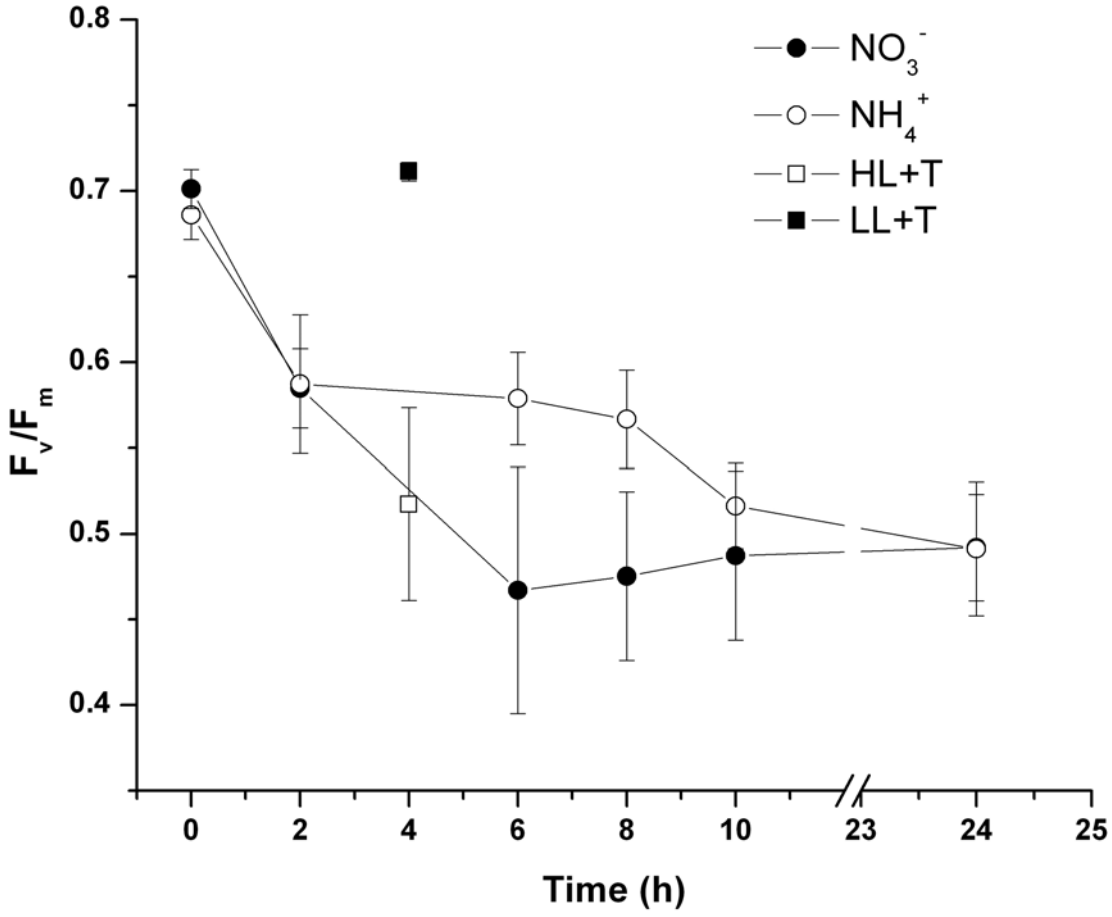

Figure 3.5 **Quantum yield (F_v/F_m) of *H. akashiwo* grown with either NO_3^- or NH_4^+ as the nitrogen source as measured by FIRe fluorometery. Cultures were shifted from 60 to 785 µmoles quanta $m^{-2}s^{-1}$ at time zero and fluorescence was measured over 24 hours. Sodium tungstate (T) was added to sub-cultures under high light (HL+T) and low light (LL+T) conditions and fluorescence was read four hours after the shift to high light. Error bars denote 1 ± S.D (n = 4).**

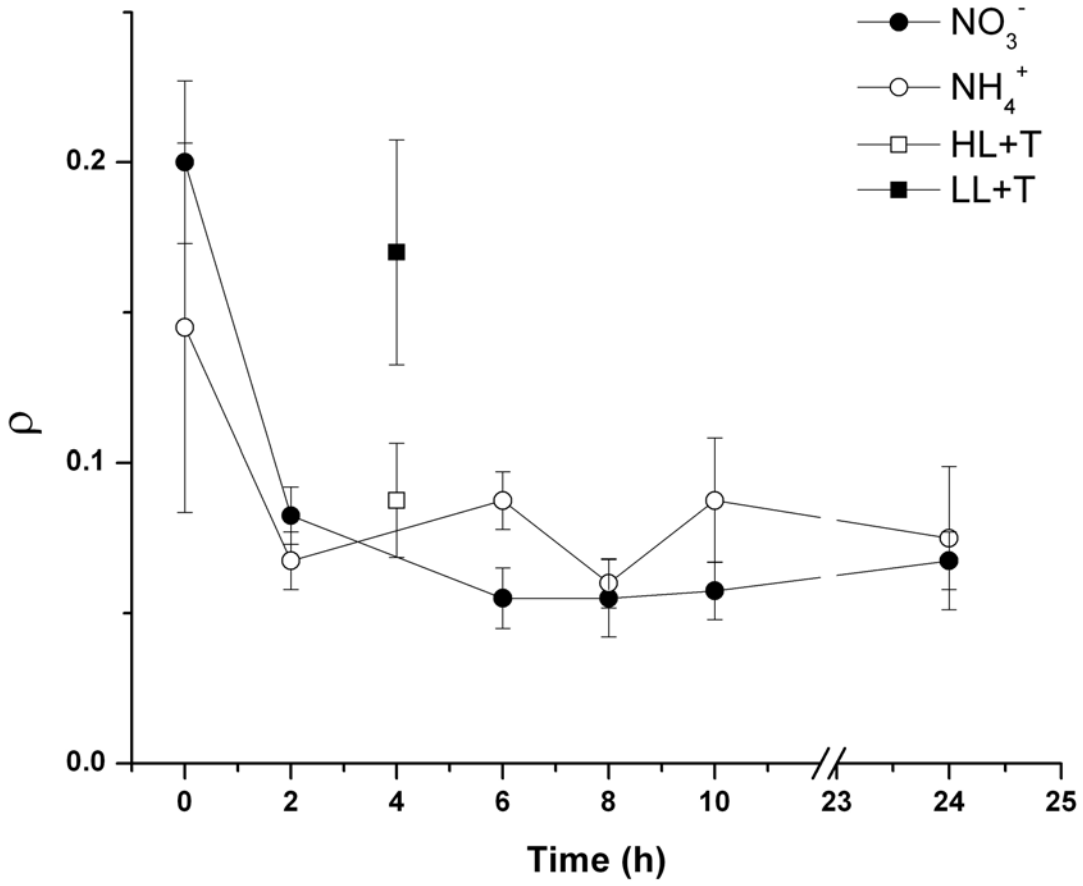

Figure 3.6 The connectivity (ρ) of PSII of cells grown on NO_3^- or NH_4^+ as measured by FIRe fluorometery. Cultures were shifted from 60 to 785 µmol quanta m^{-2} s^{-1} at time zero. Sodium tungstate (T) was added to sub-cultures under high light (HL + T) and low light (LL + T) conditions and fluorescence was read four hours after the shift to high light. Error bars denote n = 4 ± S.D.

3.4 Conclusions

The initial pilot study comparing *H. akashiwo* cells grown on NO_3^- or NH_4^+ under low light conditions agreed with our expectation of enhanced ETR_{max}

when cells were nitrate-replete. However, these results were not replicated in the two following studies showing no significant differences in ETR_{max} between the two nitrogen regimes and diverged even further with low light acclimated cells exhibiting transport rates an order of magnitude higher than the initial study. In the second study ETR_{max} rapidly declined during the first four hours under both nitrate and ammonium but showed no significant change whether measured by PAM or FIRe fluorometery in the third trial (Fig. 3.2 and Fig. 3.4). Additionally no significant impact of sodium tungstate on ETR_{max} was seen in any of the studies suggesting that either NR is only a short term sink for excess electrons, *H. akashiwo* does not utilize the NR pathway as a dissipation mechanism under prolonged high irradiance stress, or that other dissipation mechanisms are being employed allowing for the maintenance of the ETR_{max}. However, despite these differences the ETR_{max} measured here fell within the range of previously reported raphidophyte ETR_{max} with *C. subsalsa* (Warner and Madden 2007).

Difficulties in reconciling ETR measurements between the second two studies could also be due to the diel periodicity of NR. For example, several studies using diatom species *Thalassiosira* have noted an increase in NR activity in the middle of the light period and a second peak towards the end of the dark period (Berges et al. 1995; Vergara et al. 1998). If a similar periodicity of NR activity occurs in raphidophytes, this might cause an over or under estimation of the proportion of electron transport utilized by NR depending on the time of measurement. Another factor that could have confounded results between studies and nutrient regimes is the temperature sensitivity of NR. Temperature response curves conducted with chromophytic phytoplankton in a study by Gao et al. (2000) revealed a temperature

optimum for NR activity between 10 and 20 °C. In contrast, the growth temperature of 25 °C used here could have negatively impacted the efficiency of NR activity in *H. akashiwo*. The experimental design used in these studies also leaves open the question of whether observations of increased ETR are indicative of solely NR activity and do not give any indication of the contribution of alternative pathways such as the Mehler reactions or photorespiration. Since both oxygen evolution and the effective quantum yield, as measured by chl *a* fluorescence, are products of PSII activity, there should be little variability between the two if the majority of electron flow is used for carboxylation. Thus, by measuring O_2 production or ^{14}C assimilation along with chl *a* fluorescence any lack of linearity between the two could indicate excess electron flow beyond carbon fixation (Geel et al. 1997). Simultaneous NR activity measurements could then quantify the contribution of this pathway as an excess electron sink.

Further work investigating the possible use of the NR pathway as an electron sink in *H. akashiwo* should also take into account the differences between PAM and FIRe methodology. Light response curves in this study derived by PAM fluorometry may have been more representative of a lower light acclimated state when compared to the FIRe protocol (100 vs. 500 µmol photons $m^{-2}s^{-1}$ actinic light, see methods). Likewise, multiple turnover saturation pulses used with the PAM fluorometer could potentially over estimate the effective quantum yield (F_v'/F_m') due to the complete reduction of the primary electron acceptor of PSII Q_A and secondary acceptor Q_B, as well as the PQ pool (Suggett et al. 2003). In comparison, single turnover chlorophyll fluorescence, such as that measured by the FIRe fluorometer, would allow for a single closure event of all PSII centers by only reducing the primary acceptor Q_A providing for a more accurate measurement of F_v'/F_m'. Although the pilot

studies presented here can not conclusively say that NR activity in *H. akashiwo* is utilized as an excess electron sink, further work should include simultaneous carbon fixation measurements, either by O_2 evolution or ^{14}C-uptake, and NR activity assays in order estimate the excess electron flow and the proportion that is utilized by NR during high light stress.

APPENDIX

Table A.1 Measured and calculated growth and carbon chemistry parameters under each of the four temperature/CO_2 treatments. Different letters denote significant difference (numbers in parenthesis = S.D. with n ≥ 3).

		cells/mL	Chl *a* (pg)/ cell	pH	DIC (μM)	pCO_2 (ppm)
H. akashiwo (DIB)			p = 0.157	p = 0.005	p = 0.004	p = 0.004
			x^2 = 5.206	f = 7.326	f = 7.570	f = 7.784
	Control	91959 (4004)	6.91 a (0.38)	8.52 a (0.19)	1448.44 a (101.22)	103.2 a,b (59.01)
	High CO_2	94209 (2966)	7.16 a (0.74)	8.74 a,b (0.1)	1350.69 a,b (59.27)	47.75 a,c (16.04)
	High temp	80827 (4132)	6.57 a (0.29)	8.84 b (0.03)	1274.48 b (21.64)	31.53 c (3.73)
	Combined	86476 (2205)	7.35 a (0.30)	8.46 a (0.15)	1490.39 a (75.94)	120.1 b (55.91)
H. akashiwo (WA)			p <0.002	p = 0.003	p = 0.009	p = 0.017
			f = 15.772	f = 8.210	f = 11.493	f = 5.040
	Control	58729 (3053)	9.89 a (0.46)	8.92 (0.07)	1292.15 a (33.82)	25.1 a (5.89)
	High CO_2	64680 (18181)	10.40 a (2.35)	8.50 (0.17)	1565.12 b (85.91)	115.95 a,b (71.41)
	High temp	47355 (4063)	15.71 b (1.42)	8.89 (0.26)	1292.62 a (165.84)	35.35 a (28.77)
	Combined	52823 (4165)	14.64 b (1.00)	8.47 (0.12)	1578.76 b (59.09)	120.75 b (48.20)

Table A.1 cont.

		cells/mL	Chl *a* (pg)/ cell	pH	DIC (μM)	pCO_2 (ppm)
C. subsalsa (DIB)			p = 0.437	p = 0.005	p = 0.007	p = 0.005
			f = 0.975	χ^2 = 12.86	χ^2 = 12.199	f = 13.059
	Control	22519 (2243)	24.50 a (3.17)	8.82 a (0.06)	1323.05 a (46.72)	35.33 a (8.69)
	High CO_2	16149 (16149)	26.33 a (1.89)	8.39 b (0.18)	1619.69 b (109.63)	164.8 b (93.78)
	High temp	23631 (2380)	28.77 a (5.90)	8.95 c (0.04)	1279.69 a (14.61)	22.6 c (2.91)
	Combined	22063 (1311)	27.49 a (2.40)	8.56 b (0.17)	1539.84 b (91.79)	96.575 b (49.40)

Table A.2 Significant ($p < 0.05$) intraspecific differences between control, high temperature, high CO_2, and combined treatments

Heterosigma akashiwo (DIB)	P_{Bmax}	α	primary productivity	F_v/F_m	σ_{PSII}	ρ	tau	NPQ	Φ_{max}
p		< 0.02		< 0.01	< 0.04	< 0.01		< 0.01	< 0.02
f		5.65		8.54	4.21	12.46		7.8	6.4
Heterosigma akashiwo (WA)									
p	< 0.01		< 0.0003	< 0.001	<0.01	<0.03		< 0.001	
f	8.19		16.32	12.84	10.17			16.71	
χ^2						9.77			
Chattonella subsalsa (DIB)									
p	< 0.01	< 0.03	< 0.01	< 0.00005	< 0.01		<0.02	<0.001	<0.02
f	7.19	4.76		19.42			5.27	16.8	5.71
χ^2			11.49		13.06				

Units: PBmax and primary productivity (µg C (µg Chl a)-1h-1, α (µg C (µg Chl a)-1 (µmol m -2s-1)-1, Φmax (mol C (mol quanta)-1

Table A.3 Significant ($p < 0.05$) interspecific differences between *Heterosigma akashiwo* (DIB), *Heterosigma akashiwo* (WA), and *Chattonella subsalsa* (DIB) grown under four treatments: 'Control' (25 °C + 375 ppm CO_2), 'High CO_2' (25 °C + 750 ppm CO_2), 'High Temperature' (30 °C + 375 ppm CO_2), 'Combined' (30 °C + 750 ppm CO_2).

		μ	P_{Bmax}	α	Prim prod
Control	p	< 0.001	< 0.001	< 0.01	< 0.01
	f	23.93	19.44	9.67	13.69
High CO_2	p	< 0.01		<0.01	<0.02
	f	17.00		16.49	
	X^2				8.91
High	p	< 0.00001		< 0.001	< 0.0001
Temperature	f	80.16		23.18	47.16
Combined	p	< 0.0001		< 0.02	< 0.001
	f	49.71		8.68	21.86

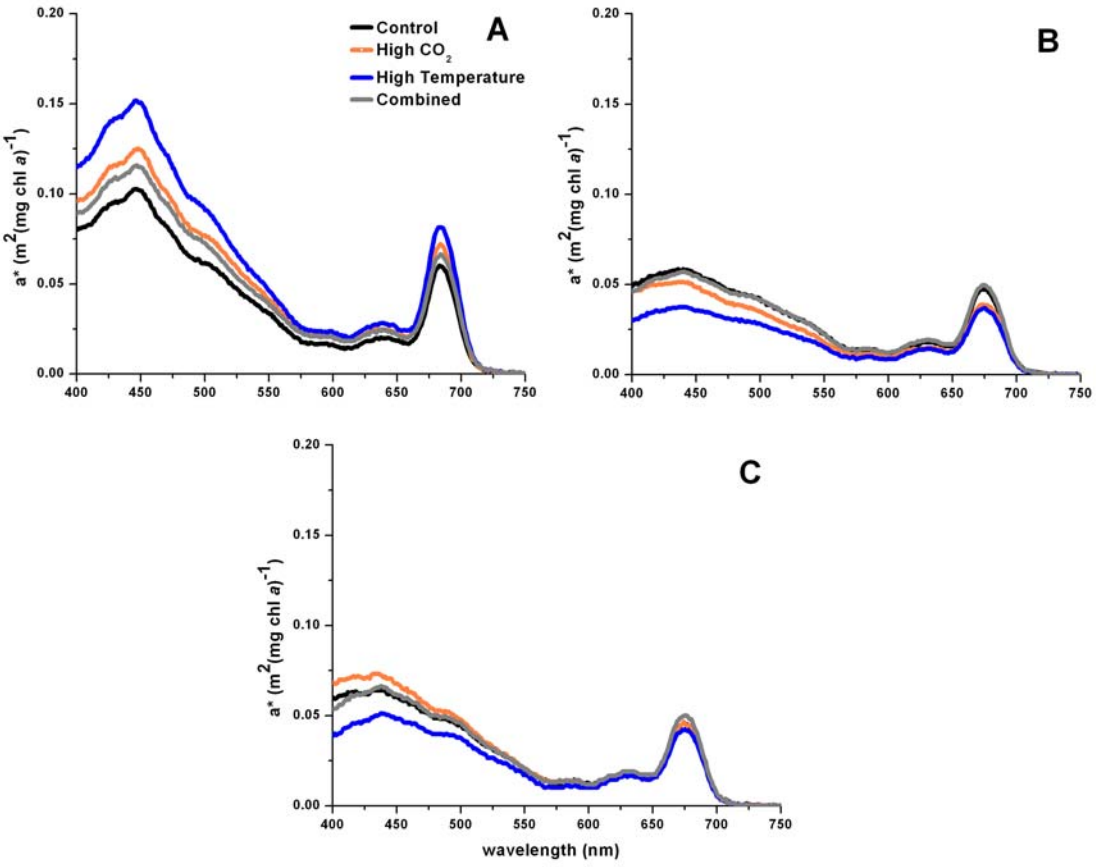

Figure A.1 **Spectral absorption for *H. akashiwo* (DIB) (A), *H. akashiwo* (WA) (B), and *C. subsalsa* (DIB) (C) under the four temperature and CO_2 treatments. Lines represent averages of four replicates.**

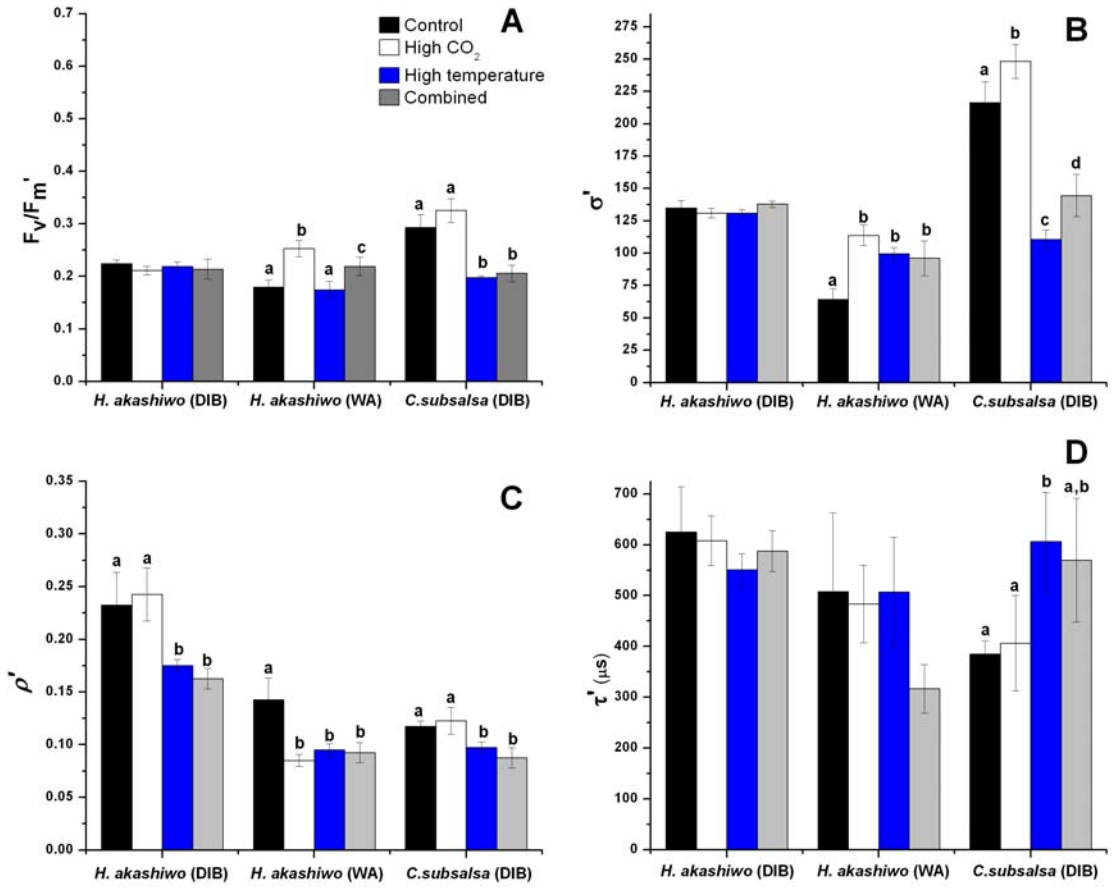

Figure A.2 **Light acclimated measurements of PSII maximal efficiency (A), functional absorption cross section (B), connectivity (C), and the rate of PSII reoxidation (D) in *H. akashiwo* (DIB), *H. akashiwo* (WA), and *C. subsalsa* (DIB). Error bars denote standard deviation (n = 3) and different letters represent significant difference within algae (One-way ANOVA, $p < 0.05$). Note: Fv'/Fm' and σ_{PSII}' were analyzed with FIRePro and ρ' and τ' were analyzed with FIReWorx.**

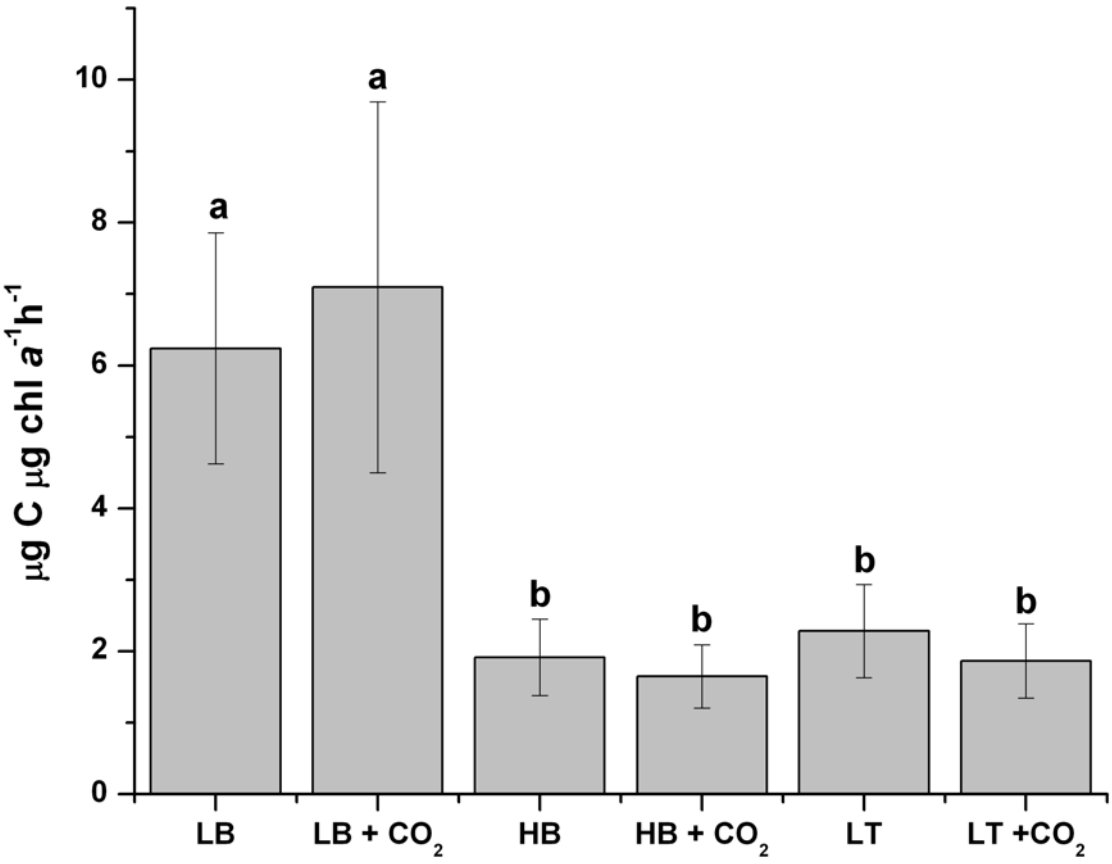

Figure A.3 **Chlorophyll *a* based carbon assimilation of *H. akashiwo* (DIB) grown under 25 °C and bubbled with ambient air (375 ppm CO_2) or high CO_2 (750 ppm CO_2). LB = low biomass, HB = high biomass, and LT = long term experiment.**

Table A.4 Measured and calculated parameters of low biomass (LB) or high biomass (HB) *H. akashiwo* (DIB) cultures bubbled with ambient air (375 ppm) or high CO_2 (750 ppm) and grown at 25 °C . Different letters denote significant difference (numbers in parentheses = S.D, n = 3).

	cells/mL	Chl *a* (pg)/ cell	pH	DIC (μM)	pCO_2 (ppm)
			$p < 0.00001$	$p < 0.0001$	$p < 0.00001$
			$f = 59.62$	$f = 45.24$	$f = 59.46$
LB	49473 (952)	34.83 a (3.00)	8.37 a (0.07)	1448.75 a (37.95)	141.0 a (27.22)
LB + CO_2	59284 (1806)	39.92 a (6.80)	8.64 b (0.07)	1336.23 b (38.69)	60.73 b (13.76)
HB	74912 (3032)	46.12 a (4.62)	9.04 c (0.05)	1106.65 c (29.93)	14.40 c (3.20)
HB + CO_2	86037 (2790)	47.30 a (4.06)	8.74 b (0.05)	1329.14 b (40.13)	45.53 b (9.03)

BIBLIOGRAPHY

Adolf JE, Stoecker DK, Harding LW (2003) Autotrophic growth and photoacclimation in *Karlodinium micrum* (Dinophyceae) and *Storeatula major* (Cryptophyceae). Journal of Phycology 39: 1101-1108

Anderson DM (1989) Toxic algal blooms and red tides: A global perspective. Elsevier, New York

Anderson DM, Glibert PM, Burkholder JM (2002) Harmful algal blooms and eutrophication: Nutrient sources, composition, and consequences. Estuaries 25: 704-726

Anderson DM, Kaoru Y, White AW (2000) Estimated Annual Economic Impacts from Harmful Algal Blooms (HABs) in the United States, Technical Report WHOI-2000-11. Woods Hole Oceanographic Institute, Woods Hole, Mass

Anning T, Harris G, Geider RJ (2001) Thermal acclimation in the marine diatom *Chaetoceros calcitrans* (Bacillariophyceae). European Journal of Phycology 36: 233-241

Anning T, MacIntyre HL, Pratt SM, Sammes PJ, Gibb S, Geider RJ (2000) Photoacclimation in the marine diatom *Skeletonema costatum*. Limnology and Oceanography 45: 1807-1817

Apel K, Hirt H (2004) REACTIVE OXYGEN SPECIES: Metabolism, Oxidative Stress, and Signal Transduction. Annual Review of Plant Biology 55: 373-399

Asada K (1999) THE WATER-WATER CYCLE IN CHLOROPLASTS: Scavenging of Active Oxygens and Dissipation of Excess Photons. Annual Review of Plant Physiology and Plant Molecular Biology 50: 601-639

Asada K (2000) The Water-Water Cycle as Alternative Photon and Electron Sinks. Philosophical Transactions: Biological Sciences 355: 1419-1431

Atkin OK, Tjoelker MG (2003) Thermal acclimation and the dynamic response of plant respiration to temperature. Trends in Plant Science 8: 343-351

Badger MR, Andrews TJ, Whitney SM, Ludwig M, Yellowlees DC, Leggat W, Price GD (1998) The diversity and coevolution of Rubisco, plastids, pyrenoids, and chloroplast-based CO2-concentrating mechanisms in algae. Natl Research Council Canada, pp 1052-1071

Baker NR (2008) Chlorophyll fluorescence: A probe of photosynthesis in vivo. Annual Review of Plant Biology 59: 89-113

Berges JA, Cochlan WP, Harrison PJ (1995) Laboratory and field responses of algal nitrate reductase to diel periodicity in irradiance, nitrate exhaustion, and the presence of ammonium. Marine Ecology-Progress Series 124: 259-269

Berner T, Dubinsky Z, Wyman K, Falkowski PG (1989) Photoadaptation and the package effect in *Dunaliella tertiolecta* (Chlorophyceae). Journal of Phycology 25: 70-78

Bourdelais AJ, Tomas CR, Naar J, Kubanek J, Baden DG (2002) New fish-killing alga in coastal Delaware produces neurotoxins. Environmental Health Perspectives 110: 465-470

Burns RA, MacDonald CD, McGinn PJ, Campbell DA (2005) Inorganic carbon repletion disrupts photosynthetic acclimation to low temperature in the cyanobacterium *Synechococcus elongatus*. Journal of Phycology 41: 322-334

Butler WL (1978) Energy-distribution in photo-chemical apparatus of photosynthesis. Annual Review of Plant Physiology and Plant Molecular Biology 29: 345-378

Casareto BE, Niraula MP, Fujimura H, Suzuki Y (2009) Effects of carbon dioxide on the coccolithophorid *Pleurochrysis carterae* in incubation experiments. Aquatic Biology 7: 59-70

Chow WS, Lee HY, He J, Hendrickson L, Hong YN, Matsubara S (2005) Photoinactivation of Photosystem II in leaves. Photosynthesis Research 84: 35-41

Clark DR, Flynn KJ (2000) The relationship between the dissolved inorganic carbon concentration and growth rate in marine phytoplankton. Proceedings of the Royal Society of London Series B-Biological Sciences 267: 953-959

Cleveland JS, Weidemann AD (1993) Quantifying Absorption by Aquatic Particles - A Multiple-Scattering Correction for Glass-Fiber Filters. Limnology and Oceanography 38: 1321-1327

Coles JF, Jones RC (2000) Effect of temperature on photosynthesis-light response and growth of four phytoplankton species isolated from a tidal freshwater river. Journal of Phycology 36: 7-16

Collins S, Bell G (2006) Evolution of natural algal populations at elevated CO_2. Ecology Letters 9: 129-135

Connell LB (2000) Nuclear ITS region of the alga Heterosigma akashiwo (Chromophyta : Raphidophyceae) is identical in isolates from Atlantic and Pacific basins. Marine Biology 136: 953-960

Czerny J, Ramos JBE, Riebesell U (2009) Influence of elevated CO_2 concentrations on cell division and nitrogen fixation rates in the bloom-forming cyanobacterium *Nodularia spumigena*. Biogeosciences 6: 1865-1875

Delille B, Harlay J, Zondervan I, Jacquet S, Chou L, Wollast R, Bellerby RGJ, Frankignoulle M, Borges AV, Riebesell U, Gattuso JP (2005) Response of primary production and calcification to changes of pCO_2 during experimental blooms of the coccolithophorid *Emiliania huxleyi*. Global Biogeochemical Cycles 19: 14

Demmig-Adams B (1990) Carotenoids and photoprotection in plants: A role for the xanthophyll zeaxanthin. Biochimica et Biophysica Acta (BBA) - Bioenergetics 1020: 1-24

Dickson AG (1990) Standard potential of the reaction: AgCl (s) $+{}^1/_2$ H_2 (g) = Ag (s) + HCL (aq), and the standard acidity constant of the ion HSO_4^- in synthetic sea

water from 273.15 to 318.15 K. Journal of Chemical Thermodynamics 22: 113-127

Dijkman NA, Kroon BMA (2002) Indications for chlororespiration in relation to light regime in the marine diatom *Thalassiosira weissflogii*. Journal of Photochemistry and Photobiology B: Biology 66: 179-187

Egge JK, Thingstad TF, Larsen A, Engel A, Wohlers J, Bellerby RGJ, Riebesell U (2009) Primary production during nutrient-induced blooms at elevated CO_2 concentrations. Biogeosciences 6: 877-885

Engel A, Delille B, Jacquet S, Riebesell U, Rochelle-Newall E, Terbruggen A, Zondervan I (2004) Transparent exopolymer particles and dissolved organic carbon production by *Emiliania huxleyi* exposed to different CO_2 concentrations: a mesocosm experiment. Aquatic Microbial Ecology 34: 93-104

Engel A, Schulz KG, Riebesell U, Bellerby R, Delille B, Schartau M (2008) Effects of CO_2 on particle size distribution and phytoplankton abundance during a mesocosm bloom experiment (PeECE II). Biogeosciences 5: 509-521

Falkowski P, Scholes RJ, Boyle E, Canadell J, Canfield D, Elser J, Gruber N, Hibbard K, Hogberg P, Linder S, Mackenzie FT, Moore B, Pedersen T, Rosenthal Y, Seitzinger S, Smetacek V, Steffen W (2000) The global carbon cycle: A test of our knowledge of earth as a system. Science 290: 291-296

Falkowski PG, Raven JA (2007) Aquatic Photosynthesis. Princeton University Press, Princeton, NJ

Feng Y, Warner ME, Zhang Y, Sun J, Fu FX, Rose JM, Hutchins DA (2008) Interactive effects of increased pCO_2, temperature and irradiance on the marine coccolithophore *Emiliania huxleyi* (Prymnesiophyceae). European Journal of Phycology 43: 87-98

Feng YY, Hare CE, Leblanc K, Rose JM, Zhang YH, DiTullio GR, Lee PA, Wilhelm SW, Rowe JM, Sun J, Nemcek N, Gueguen C, Passow U, Benner I, Brown C, Hutchins DA (2009) Effects of increased pCO_2 and temperature on the North Atlantic spring bloom. I. The phytoplankton community and biogeochemical response. Marine Ecology-Progress Series 388: 13-25

Friederich GE, Walz PM, Burczynski MG, Chavez FP (2002) Inorganic carbon in the central California upwelling system during the 1997-1999 El Niño-La Niña event. Progress In Oceanography 54: 185-203

Fu FX, Warner ME, Zhang YH, Feng YY, Hutchins DA (2007) Effects of increased temperature and CO_2 on photosynthesis, growth, and elemental ratios in marine *Synechococcus* and *Prochlorococcus* (Cyanobacteria). Journal of Phycology 43: 485-496

Fu FX, Zhang YH, Warner ME, Feng YY, Sun J, Hutchins DA (2008) A comparison of future increased CO_2 and temperature effects on sympatric *Heterosigma akashiwo* and *Prorocentrum minimum*. Harmful Algae 7: 76-90

Gao KS, Guan WC, Helbling EW (2007) Effects of solar ultraviolet radiation on photosynthesis of the marine red tide alga *Heterosigma akashiwo* (Raphidophyceae). Journal of Photochemistry and Photobiology B-Biology 86: 140-148

Gao Y, Smith GJ, Alberte RS (2000) Temperature dependence of nitrate reductase activity in marine phytoplankton: Biochemical analysis and ecological, implications. Journal of Phycology 36: 304-313

Geel C, Versluis W, Snel JFH (1997) Estimation of oxygen evolution by marine phytoplankton from measurement of the efficiency of Photosystem II electron flow. Photosynthesis Research 51: 61-70

Gordillo FJL, Jimenez C, Figueroa FL, Niell FX (2003) Influence of elevated CO2 and nitrogen supply on the carbon assimilation performance and cell composition of the unicellular alga *Dunaliella viridis*. Physiologia Plantarum 119: 513-518

Hallegraeff GM (1993) A review of harmful algal blooms and their apparent global increase. Phycologia 32: 79-99

Hallegraeff GM (2003) Harmful algal blooms: a global overview. In: Hallegraeff GM, Anderson DM, Cembella AD, Enevoldsen HO (eds) Manual on Harmful Marine Microalgae. Unesco, Paris, pp 25-49

Hallegraeff GM, Hara Y (2003) Taxonomy of harmful marine raphidophytes. In: Hallegraeff GM, Anderson DM, Cembella AD, Enevoldsen HO (eds) Manual on Harmful Marine Microalgae. Unesco, Paris, pp 511 - 522

Handy SM, Coyne KJ, Portune KJ, Demir E, Doblin MA, Hare CE, Cary SC, Hutchins DA (2005) Evaluating vertical migration behavior of harmful raphidophytes in the Delaware Inland Bays utilizing quantitative real-time PCR. Aquatic Microbial Ecology 40: 121-132

Harris GN, Scanlan DJ, Geider RJ (2005) Acclimation of *Emiliania huxleyi* (Prymnesiophyceae) to photon flux density. Journal of Phycology 41: 851-862

HARRNESS (2005) Harmful Algal Research and Response: A National Environmental Science Strategy 2005 – 2015, Washington DC

Herndon J, Cochlan WP (2007) Nitrogen utilization by the raphidophyte *Heterosigma akashiwo*: Growth and uptake kinetics in laboratory cultures. Harmful Algae 6: 260-270

Honjo T (1991) Overview on bloom dynamics and physiological ecology of *Heterosigma akashiwo*. In: Smayda TJ, Shimizu Y (eds) Fifth International Conference on Toxic Marine Phytoplankton. Elsevier, Newport, Rhode Island

Hurd CL, Hepburn CD, Currie KI, Raven JA, Hunter KA (2009) Testing the effects of ocean acidification on algal metabolism: Considerations for experimental designs Journal of Phycology 45: 1236-1251

Hutchins DA, Fu FX, Zhang Y, Warner ME, Feng Y, Portune K, Bernhardt PW, Mulholland MR (2007) CO2 control of Trichodesmium N-2 fixation, photosynthesis, growth rates, and elemental ratios: Implications for past,

present, and future ocean biogeochemistry. Limnology and Oceanography 52: 1293-1304
IPCC (2007) Summary for Policymakers. In: Solomon S, Qin D, Manning M, Chen Z, Marquis M, Averyt KB, Tignor M, Miller HL (eds) Climate Change 2007: Contribution of Working Groups I, II and III to the Fourth Assessment Report of the Intergovernmental Panel on Climate Change [Core Writing Team, Pachauri, R.K and Reisinger, A. (eds.)]. Cambridge University Press, Cambridge, United Kingdom and New York, NY, USA
Jassby AD, Platt T (1976) Mathmatical formulation of relationship between photosynthesis and light for phytoplankton. Limnology and Oceanography 21: 540-547
Jones LW, Kok B (1966) Photoinhibition of chloroplast reactions. I. Kinetics and action spectra. Plant Physiology 41: 1037-&
Kemp WM, Boynton WR, Adolf JE, Boesch DF, Boicourt WC, Brush G, Cornwell JC, Fisher TR, Glibert PM, Hagy JD, Harding LW, Houde ED, Kimmel DG, Miller WD, Newell RIE, Roman MR, Smith EM, Stevenson JC (2005) Eutrophication of Chesapeake Bay: historical trends and ecological interactions. Marine Ecology-Progress Series 303: 1-29
Keppler CJ, Lewitus AJ, Ringwood AH, Hoguet J, Staton T (2006) Sublethal cellular effects of short-term raphidophyte and brevetoxin exposures on the eastern oyster *Crassostrea virginica*. Marine Ecology-Progress Series 312: 141-147
Khan S, Arakawa O, Onoue Y (1997) Neurotoxins in a toxic red tide of *Heterosigma akashiwo* (Raphidophyceae) in Kagoshima Bay, Japan. Aquaculture Research 28: 9-14
Kim D, Watanabe M, Nakayasu Y, Kohata K (2004) Production of superoxide anion and hydrogen peroxide associated with cell growth of *Chattonella antiqua*. Aquatic Microbial Ecology 36: 311-311
Langdon C, Takahashi T, Sweeney C, Chipman D, Goddard J, Marubini F, Aceves H, Barnett H, Atkinson MJ (2000) Effect of calcium carbonate saturation state on the calcification rate of an experimental coral reef. Global Biogeochemical Cycles 14: 639-654
Levitan O, Rosenberg G, Setlik I, Setlikova E, Grigel J, Klepetar J, Prasil O, Berman-Frank I (2007) Elevated CO_2 enhances nitrogen fixation and growth in the marine cyanobacterium *Trichodesmium*. Global Change Biology 13: 531-538
Li YH, Takahash.T, Broecker WS (1969) Degree of saturation of $CaCO_3$ in oceans. Journal of Geophysical Research 74: 5507-&
Lomas MW, Glibert PM (1999) Temperature regulation of nitrate uptake: A novel hypothesis about nitrate uptake and reduction in cool-water diatoms. Limnology and Oceanography 44: 556-572
MacIntyre HL, Kana TM, Geider RJ (2000) The effect of water motion on short-term rates of photosynthesis by marine phytoplankton. Trends in Plant Science 5: 12-17

Makino A, Miyake C, Yokota A (2002) Physiological Functions of the Water-Water Cycle (Mehler Reaction) and the Cyclic Electron Flow around PSI in Rice Leaves. Plant Cell Physiol. 43: 1017-1026

Marshall JA, Newman S (2002) Differences in photoprotective pigment production between Japanese and Australian strains of *Chattonella marina* (Raphidophyceae). Journal of Experimental Marine Biology and Ecology 272: 13-27

Maxwell DP, Falk S, Trick CG, Huner NPA (1994) Growth at low temperature mimics high-light acclimation in *Chlorella vulgaris*. Plant Physiology 105: 535-543

Maxwell DP, Laudenbach DE, Huner NPA (1995) Redox regulation of light-harvesting complex II and cab mRNA abundance in *Dunaliella salina*. Plant Physiol. 109: 787-795

Michaloudi E, Moustaka-Gouni M, Gkelis S, Pantelidakis K (2009) Plankton community structure during an ecosystem disruptive algal bloom of *Prymnesium parvum*. Journal of Plankton Research 31: 301-309

Miyagi N, Satoh S, Fujii T (1992) A nitrate-inducible plasma membrance protein of a marine alga, *Heterosigma akashiwo*. Plant and Cell Physiology 33: 971-976

Nimer NA, Iglesias-Rodriguez MD, Merrett MJ (1997) Bicarbonate utilization by marine phytoplankton species. Journal of Phycology 33: 625-631

Oda T, Ishimatsu A, Takeshita S, Muramatsu T (1994) Hydrogen peroxide production by the red tide flagellate *Chattonella marina*. Bioscience Biotechnology and Biochemistry 58: 957-958

Oda T, Nakamura A, Shikayama M, Kawano I, Ishimatsu A, Muramatsu T (1997) Generation of reactive oxygen species by raphidophycean phytoplankton. Bioscience Biotechnology and Biochemistry 61: 1658-1662

Okaichi T (1989) Red tide problems in the Seto Inland Sea, Japan. In: Okaichi T, Anderson DM, Nemoto T (eds) International Symposium on Red Tides Elsevier, New York, pp 137 - 142

Parker MS, Armbrust EV (2005) Synergistic effects of light, temperature, and nitrogen source on transcription of genes for carbon and nitrogen metabolism in the centric diatom *Thalassiosira pseudonana* (Bacillariophyceae). Journal of Phycology 41: 1142-1153

Peltier G, Cournac L (2002) Chlororespiration. Annual Review of Plant Biology 53: 523-550

Platt T, Gallegos CL, Harrison WG (1980) Photoinhibition of photosynthesis in natural assemblages of marine phytoplankton. Journal of Marine Research 38: 687-701

Portis AR, Parry MAJ (2007) Discoveries in Rubisco (Ribulose 1,5-bisphosphate carboxylase/oxygenase): a historical perspective. Photosynthesis Research 94: 121-143

Pospisil P, Tyystjarvi E (1999) Molecular mechanism of high-temperature-induced inhibition of acceptor side of Photosystem II. Photosynthesis Research 62: 55-66

Post AF, Dubinsky Z, Wyman K, Falkowski PG (1984) Kinetics of light intensity adaptation in a marine planktonic diatom. Marine Biology 83: 231-238

Raven JA (1991) Physiology of inorganic C acquisition and implications for resource use efficiency by marine phytoplankton - Relation to increases CO_2 and temperature. Plant Cell and Environment 14: 779-794

Raven JA, Geider RJ (1988) Temperature and algal growth. New Phytologist 110: 441-461

Rensel JEJ (2007) Fish Kills from the harmful alga *Heterosigma akashiwo* in Puget Sound: Recent blooms and review. Rensel Associates Aquatic Sciences, Arlington, Washington

Riebesell U (2004) Effects of CO_2 enrichment on marine phytoplankton. Journal of Oceanography 60: 719-729

Riebesell U, Schulz KG, Bellerby RGJ, Botros M, Fritsche P, Meyerhofer M, Neill C, Nondal G, Oschlies A, Wohlers J, Zollner E (2007) Enhanced biological carbon consumption in a high CO_2 ocean. Nature 450: 545-U510

Riebesell U, Wolfgladrow DA, Smetacek V (1993) Carbon dioxide limitation of marine phytoplankton growth rates. Nature 361: 249-251

Riebesell U, Zondervan I, Rost B, Tortell PD, Zeebe RE, Morel FMM (2000) Reduced calcification of marine plankton in response to increased atmospheric CO_2. Nature 407: 364-367

Rose JM, Feng YY, Gobler CJ, Gutierrez R, Hare CE, Leblanc K, Hutchins DA (2009) Effects of increased pCO_2 and temperature on the North Atlantic spring bloom. II. Microzooplankton abundance and grazing. Marine Ecology-Progress Series 388: 27-40

Rost B, Riebesell U, Burkhardt S, Sultemeyer D (2003) Carbon acquisition of bloom-forming marine phytoplankton. Limnology and Oceanography 48: 55-67

Rost B, Zondervan I, Wolf-Gladrow D (2008) Sensitivity of phytoplankton to future changes in ocean carbonate chemistry: current knowledge, contradictions and research directions. Marine Ecology Progress Series 373: 227-237

Salvucci ME, Crafts-Brandner SJ (2004) Inhibition of photosynthesis by heat stress: the activation state of Rubisco as a limiting factor in photosynthesis. Physiologia Plantarum 120: 179-186

Schippers P, Lurling M, Scheffer M (2004) Increase of atmospheric CO_2 promotes phytoplankton productivity. Ecology Letters 7: 446-451

Schulz KG, Ramos JBE, Zeebe RE, Riebesell U (2009) CO_2 perturbation experiments: similarities and differences between dissolved inorganic carbon and total alkalinity manipulations. Biogeosciences 6: 2145-2153

Schulz KG, Riebesell U, Bellerby RGJ, Biswas H, Meyerhofer M, Muller MN, Egge JK, Nejstgaard JC, Neill C, Wohlers J, Zollner E (2008) Build-up and decline of organic matter during PeECE III. Biogeosciences 5: 707-718

Shi D, Xu Y, Morel FMM (2009) Effects of the pH/pCO_2 control method on medium chemistry and phytoplankton growth. Biogeosciences 6: 1199-1207

Spalding MH, Van K, Wang Y, Nakamura Y (2002) Acclimation of *Chlamydomonas* to changing carbon availability. Functional Plant Biology 29: 221-230

Staehr PA, Birkeland MJ (2006) Temperature acclimation of growth, photosynthesis and respiration in two mesophilic phytoplankton species. Phycologia 45: 648-656

Staehr PA, Sand-Jensen K (2006) Seasonal changes in temperature and nutrient control of photosynthesis, respiration and growth of natural phytoplankton communities. Freshwater Biology 51: 249-262

Staubitz WW, Bortleson GC, Semans SD, Tesoriero AJ, Black RW (1997) Water-Quality Assessment of the Puget Sound Basin, Washington, Environmental Setting and Its Implications for Water Quality and Aquatic Biota. US Geological Survey Water Resources Investigations Report, 97-4013

Suggett DJ, Moore CM, Marañón E, Omachi C, Varela RA, Aiken J, Holligan PM (2006) Photosynthetic electron turnover in the tropical and subtropical Atlantic Ocean. Deep Sea Research Part II: Topical Studies in Oceanography 53: 1573-1592

Suggett DJ, Oxborough K, Baker NR, MacIntyre HL, Kana TM, Geider RJ (2003) Fast repetition rate and pulse amplitude modulation chlorophyll a fluorescence measurements for assessment of photosynthetic electron transport in marine phytoplankton. European Journal of Phycology 38: 371-384

Suggett DJ, Warner ME, Smith DJ, Davey P, Hennige S, Baker NR (2008) Photosynthesis and production of hydrogen peroxide by *Symbiodinium* (Pyrrhophyta) phylotypes with different thermal tolerances. Journal of Phycology 44: 948-956

Sunda WG, Graneli E, Gobler CJ (2006) Positive feedback and the development and persistence of ecosystem disruptive algal blooms. Journal of Phycology 42: 963-974

Tilman D (1977) Resource competition between planktonic algae: An experimental and theoretical approach. Ecology 58: 338-348

Tortell PD, Rau GH, Morel FMM (2000) Inorganic carbon acquisition in coastal Pacific phytoplankton communities. Limnology and Oceanography 45: 1485-1500

Twiner MJ, Dixon SJ, Trick CG (2001) Toxic effects of *Heterosigma akashiwo* do not appear to be mediated by hydrogen peroxide. Limnology and Oceanography 46: 1400-1405

Twiner MJ, Trick CG (2000) Possible physiological mechanisms for production of hydrogen peroxide by the ichthyotoxic flagellate *Heterosigma akashiwo*. Journal of Plankton Research 22: 1961-1975

Vergara JJ, Berges JA, Falkowski PG (1998) Diel periodicity of nitrate reductase activity and protein levels in the marine diatom *Thalassiosira weissflogii* (Bacillariophyceae). Journal of Phycology 34: 952-961

Vu JCV, Allen LH, Boote KJ, Bowes G (1997) Effects of elevated CO_2 and temperature on photosynthesis and Rubisco in rice and soybean. Plant Cell and Environment 20: 68-76

Warner ME, Madden ML (2007) The impact of shifts to elevated irradiance on the growth and photochemical activity of the harmful algae *Chattonella subsalsa* and *Prorocentrum minimum* from Delaware. Harmful Algae 6: 332-342

Yang CZ, Albright LJ (1992) Effects of the harmful diatom *Chaetoceros concavicornis* on respiration of rainbow trout *Oncorhynchus mykiss*. Diseases of Aquatic Organisms 14: 105-114

Zeebe RE, Wolf-Gladrow D (2001) CO_2 in Seawater: Equilibrium, Kinetics, Isotopes. Elsevier, Amsterdam

Zhang YH, Fu FX, Whereat E, Coyne KJ, Hutchins DA (2006) Bottom-up controls on a mixed-species HAB assemblage: A comparison of sympatric *Chattonella subsalsa* and *Heterosigma akashiwo* (Raphidophyceae) isolates from the Delaware Inland Bays, USA. Harmful Algae 5: 310-320